2019

Blubber transcriptome and proteome responses to repeated adrenocorticotropic hormone administration in a marine mammal

Jared Deyarmin
University of the Pacific

BLUBBER TRANSCRIPTOME AND PROTEOME RESPONSES TO REPEATED ADRENOCORTICOTROPIC HORMONE ADMINISTRATION IN A MARINE MAMMAL

by

Jared S. Deyarmin

A Thesis Submitted to the

Graduate School

in Partial Fulfillment of the

Requirements for the Degree of

MASTER OF SCIENCE

College of the Pacific
Biological Sciences

University of the Pacific,
Stockton, California

2019

BLUBBER TRANSCRIPTOME AND PROTEOME RESPONSES TO REPEATED ADRENOCORTICOTROPIC HORMONE ADMINISTRATION IN A MARINE MAMMAL

by

Jared S. Deyarmin

APPROVED BY:

Thesis Advisor: Jane Khudyakov, Ph.D.

Committee Member: Craig Vierra, Ph.D.

Committee Member: Zachary Stahlschmidt, Ph.D.

Department Chair: Eric Thomas, Ph.D.

Dean of Graduate School: Thomas H. Naehr, Ph.D.

DEDICATION

This thesis is dedicated to my love for science, biology, and quenching my thirst for knowledge in a subject I am passionate for. I struggled to develop my interests in biology as I was set on a healthcare career path, but with the help of friends and various faculty from my undergraduate education, I happily found a more appropriate fit in research and applied biology. Education has been nothing but an exhilarating journey for me. My life has changed following something I am passionate about, and I'd like to thank those who helped me find this path. I would not be here without the support of one of my closest friends, Daniel Atencio, for motivating me to exceed expectations and chase my dreams. He has been there for me through all of my struggles and has always instilled living an authentic life, as well as inspiring me to be true to myself. I was the first one to explore higher education in my family and it put me in a position where I faced controversies along the way. With your support and our conversations, those controversies were easily looked over. In addition, this thesis is dedicated to my grandmother, Willa-Mae Deyarmin. She was the main person in my family that provided the emotional and psychological support I needed, and I wish she could be here to see what I've accomplished. In all, I would not be here without the support of my family. Even though education was outside of their wheelhouse, they still supported me living an authentic life, pursuing my dreams, and supported me until I was able to support myself. Thank you, all; I made it.

ACKNOWLEDGEMENTS

I want to acknowledge everyone who helped me get here, as well as many of the people who helped me with this specific project. Kevin Roberts, you compelled me to pursue research while I was an undergraduate at Sonoma State University. At that point in my educational career, I had no interest in research as I never saw the importance of how research contributed to biology outside of relevant coursework. With the assistance of Kevin Roberts, I was able to find my passion for research, commit to an honor's undergraduate thesis, and graduate with distinction as research fueled my thirst for knowledge in applied biology. Lastly, I'd like to thank Mikayla Shanafelt for putting up with my nonsense and countless hours spent listening to my complaining and reading over drafts of my writing. You have been vital in my growth here at Pacific and the communal passion we share for science, research, food, and life itself has been the best emotional support I have needed.

I would also like to thank my graduate school thesis committee: Drs. Craig Vierra and Zachary Stahlschmidt. With their support, I was able to push harder, expand my knowledge across many disciplines in biology, open many collaborations across multiple labs at the University of the Pacific, and find my niche. Whether it be talking about conspiracies and mass spectrometry projects with Dr. Vierra, or shooting many research ideas out in the air and forwarding my conceptual understanding of personal, academic, and the balance in life around me with Dr. Stahlschmidt, you two have helped and motivated me throughout my years at Pacific.

Lastly, I would like to acknowledge Dr. Jane Khudyakov, my graduate school thesis advisor. I came to the University of the Pacific knowing Jane from Sonoma State University.

Upon the invitation to work in her lab, I knew she was the perfect fit for me as I admired her dedication as a scientist. Working and collaborating with Jane has been an amazing experience to say at the least. I thought I could "science" until I got here, and with the assistance from Jane, I now feel like I have the ability to be an established scientist. Ever since I walked through her door, Jane has put me as one of her top priorities and has spent countless of hours helping me with my research and writing. Jane tailored her guidance to align with my career goals. With that in mind, she figured out the best advisement style and helped me persevere in achieving my ambitions. Working closely with her has taught me a plethora of techniques, how to be a credible scientist, and I know I would not be leaving Pacific with near as many skills if it wasn't for her. The dedication she has towards her studies has pushed me harder than ever, and I can't thank her enough for what she has done for me. After working for her for three years, I aspire to be as thorough and articulated as a scientist as she is in my scientific career.

Finally, I'd like to acknowledge that our research was supported by Office of Naval Research Award number N00014-15-1-2773 to C. D. Champagne, J. I. Khudyakov, D. E. Crocker, and D. S. Houser.

To all, the words thank you hardly show my appreciation. I would not be here without any of you.

Blubber Transcriptome and Proteome Responses to Repeated Adrenocorticotropic Hormone Administration in a Marine Mammal

Abstract

By Jared Deyarmin

University of the Pacific
2019

Chronic physiological stress impacts animal fitness by catabolizing metabolic stores and suppressing reproduction and immunity. This can be especially deleterious for capital breeding carnivores, such as marine mammals, which rely on lipid stores accrued during intensive foraging to sustain prolonged periods of fasting associated with reproduction. Therefore, chronic stress may cause a decrease in fitness in these animals, leading to population declines and potentially detrimental shifts in food web dynamics as a result. However, the impacts and indicators of chronic stress in animals are currently poorly understood. To identify downstream mediators of repeated stress responses in marine mammals, adrenocorticotropic hormone (ACTH) was administered once daily for four days to free-ranging juvenile northern elephant seals (*Mirounga angustirostris*) to stimulate endogenous corticosteroid release. I then compared blubber tissue transcriptome responses to the first and fourth ACTH administrations to determine the effects of acute and chronic endocrine stress, respectively. Gene expression profiles showed differences in responses to single and repeated ACTH administration, despite similarities in circulating cortisol profiles. We identified 61 and 12 differentially expressed genes (DEGs) in response to the first ACTH and fourth administrations, respectively, 24 DEGs between the first and fourth pre-ACTH samples, and 12 DEGs between ACTH response samples from the first

and fourth days. Annotated DEGs were associated with functions in redox and lipid homeostasis, suggesting potential negative impacts of repeated stress on marine mammals. In addition, protein expression profiles were discrete between single and repeated ACTH administrations, and identified changes in expression of extracellular proteins that were not detected at the transcriptome level. We identified 8 and 7 differentially expressed proteins (DEPs) in response to the first and fourth ACTH administrations, respectively, including 5 DEPs in the overall ACTH response, 1 DEP between the first and fourth pre-ACTH samples, and 10 DEPs between ACTH response samples from the first and fourth days. Differentially expressed proteins in response to repeated ACTH administrations were associated with extracellular matrix (ECM) remodeling and suggest a link between glucocorticoid-induced adipogenesis and ECM remodeling in blubber. Other differentially expressed proteins were associated with increased lipid metabolism and decreased immunity, consistent with transcriptome data. Together, the use of transcriptomics and proteomics to detect responses to repeated stress provides more comprehensive insight into the marine mammal stress response and highlights the importance of using multiple discovery-driven approaches for understanding stress physiology. The gene and protein markers identified in this study may be used to identify stressed animals and discriminate between acutely and chronically stressed individuals with higher sensitivity than hormone measurements alone.

TABLE OF CONTENTS

LIST OF TABLES

Table

LIST OF FIGURES

Figure

Chapter 1: Introduction

Increasing anthropogenic activity has been associated with a loss of biodiversity in many ecosystems [2]. Consequences of anthropogenic disturbance, such as declines in apex predator populations, are causing detrimental shifts in food web dynamics [3]. For example, the collapse of large marine carnivore populations has been associated with altered trophic structure and decline of commercially valuable fish stocks [4]. According to the U.S. Marine Mammal Commission, 29 species of marine mammals are currently endangered, and 13 more are considered threatened. Marine mammal populations are threatened by noise pollution, ship strikes, fisheries competition and bycatch, prey declines, habitat loss, and climate change [5-8]. In addition to direct effects on survival, anthropogenic disturbance may have sub-lethal effects on marine mammal health, fitness, and population persistence by causing physiological stress.

The Stress Response

Stress response pathways maintain homeostasis and mediate the relationship between an animal and its external environment [9]. The mammalian stress response is mediated by the hypothalamic-pituitary-adrenal (HPA) axis [10]. In response to psychological or physiological stress, corticotropin-releasing hormone (CRH) is released by the hypothalamus, triggering the release of adrenocorticotropic hormone (ACTH) by the pituitary gland. This, in turn, stimulates the synthesis of corticosteroids (glucocorticoids and mineralocorticoids) by the adrenal glands.

Stress studies in terrestrial mammals have primarily focused on downstream effects of glucocorticoids (e.g., cortisol) rather than mineralocorticoids, but a number of studies demonstrate that the mineralocorticoid aldosterone is an important component of stress responses

in marine mammals [1, 11, 12]. Corticosteroids circulate in blood complexed with binding globulins (e.g., corticosteroid-binding globulin), and free hormones exert biological effects by binding to cell surface and intracellular receptors – glucocorticoid receptor, GR, and mineralocorticoid receptor, MR – in target tissues (e.g., adipose, muscle, and liver). Cell surface receptors alter signaling pathways, while intracellular hormone-receptor complexes translocate to the nucleus, bind glucocorticoid and mineralocorticoid response elements of target genes, and impact gene transcription [13]. Altered expression of target genes, such as those encoding metabolic enzymes and hormones, promotes the physiological adjustments required to overcome the stressor. These adjustments include mobilization of glucose and lipid stores to meet increased energy demands and transient suppression of energetically expensive processes, such as reproduction, growth, and immune responses [10]. While short-term (acute) stress responses are adaptive [14-16], repeated (chronic) stress exposure may deplete energy stores and impair immunity and reproduction, thereby reducing fitness. This could be detrimental to threatened animal populations that already experience nutritional stress and low fecundity, such as some marine mammals [17]. However, little is known about the indicators and downstream effects of repeated stress in wildlife, which hinders the ability of conservation biologists to identify stressed animals and predict the effects of repeated stress on population stability [18, 19].

Marine Mammals

Many marine mammals rely on endogenous energy reserves to support life history stages characterized by high energy expenditure and nutrient limitation. For example, most semiaquatic marine mammals (e.g., pinnipeds – seals and sea lions) reproduce on land using a capital breeding strategy, in which animals rely solely on energy stores to fuel metabolic demands of reproduction [20, 21]. Many fully aquatic marine mammals (e.g., cetaceans) are also capital

breeders that migrate long distances between foraging and breeding grounds [22]. Both examples necessitate energy accumulation and storage during feeding and energy mobilization during fasting, a process that occurs from several weeks to several months as part of marine mammal life history. The main energy depot in cetaceans and pinnipeds is blubber, a specialized type of subcutaneous adipose tissue that plays significant roles in metabolism (similarly to white adipose tissue, WAT, in other mammals) and thermoregulation. Blubber is vertically stratified into at least two layers: an outer layer used for thermoregulation, and an inner, metabolically active layer [23]. WAT is a major target of stress hormones in other mammals [24] and studies in marine mammals have shown that acute HPA axis activation mobilizes stored lipids [11, 25]. Therefore, it is plausible that chronic or repeated stress would deregulate fasting metabolism and deplete lipid stores, among other impacts, limiting the ability of capital breeders to meet the energetic demands of reproduction and leading to declines in fitness.

The Study System: Northern Elephant Seals

Northern elephant seals (*Mirounga angustirostris*) are a deep diving pinniped species that forages in the mesopelagic zone of the open ocean. They have predictable times in which they haul out (come and remain ashore) for life history stages, such as breeding in winter, as well as molting in spring and summer [26]. While ashore, elephant seals remain in a fasted state for 1 to 3 months and utilize metabolic stores (e.g. blubber) to fuel the energy demands associated with life history challenges. In addition, juveniles have an additional brief haul out period in the fall. Due to their ease of access at coastal rookeries and amenability as research subjects, they are ideal candidates for physiological studies. Extensive physiological datasets have been collected on elephant seals, making them an established marine mammal study system. Past studies have described variation in baseline hormone levels [27], responses to acute ACTH administration

[14, 25, 28, 29], and metabolic adjustments during fasting [30, 31]. In addition, anesthesia procedures have been shown to minimize handling stress in this species, enabling measurements of true baseline hormone, gene expression, and protein expression levels [32]. Therefore, the elephant seal serves as an ideal free-ranging marine mammal study system in which to examine physiological stress responses, as experimental perturbations under anesthesia do not cause handling stress in this species, and which can serve as a proxy for more endangered or less accessible marine mammals.

Omics Approaches for Marine Mammal Systems

Model organisms have been used to examine many fundamental questions across disciplines in biology [33]. This has limited our understanding of the biology of lesser-studied species, which predominately make up the Earth's biodiversity and shape the environments and food webs on which humans depend [34]. Model organisms are commonly used in research as they tend to be simple, fast-growing, and easy to manipulate in the laboratory [33]. For example, fruit flies have forwarded the understanding of genetic regulation of development, yeast has been used to study the basic aspects of eukaryotic biology, and mice have been used to understand human genetic diseases [35]. As stated in the Krogh principle, a central concept in comparative physiology and functional genomics, many biological problems will be investigated using an animal or a few animal species that are most convenient to study [36]. With the foundation and techniques provided by model system research, genome sequencing tools and other modern molecular techniques can be applied to non-model systems to answer specific biological questions that could not be addressed within constraints of model organisms [35]. However, due to limited resources and understanding of non-model organism biology and fewer scientists working on these systems, the evolution of scientific discovery has progressed at a slower rate in

non-model than model organisms [35]. Until the costs of genome sequencing declined and other tools, such as RNA sequencing (transcriptomics) and protein sequencing (proteomics) became accessible, non-model organism studies were limited as the ability to study global changes in gene or protein expression in response to experimental treatments was not possible.

Application of modern sequencing techniques to non-model system research has helped revolutionize biology by enabling rapid and large-scale discovery of molecular processes underlying phenotype and physiology [37]. RNA sequencing has allowed scientists to rapidly obtain sequence information and identify global changes in gene expression in response to biological changes without a reference genome. It also serves as the most sensitive detection method for capturing biological changes among non-targeted approaches [38]. RNA sequencing enables detection of various types of transcripts, including protein-coding transcripts, regulatory non-coding transcripts, and splice variants, but does not provide information on functional consequences of their expression [39]. Proteomics can address that limitation by identifying proteins and changes in protein abundances that are consequences of gene expression, as well as detecting secreted proteins, such as those that comprise the extracellular matrix or are released in exosomes [40]. These techniques are especially useful for comparative physiology studies as both approaches are cost-effective and allow researchers to analyze all expressed RNA or protein molecules that change in response to physiological or environmental alterations. Furthermore, they provide the ability to collect large molecular datasets rapidly for organisms in which little is known otherwise [37]. Thus, using both approaches allows for a comprehensive, non-biased approach for understanding the molecular responses of non-model organisms to physiological and environmental changes, even in the absence of sequenced genomes.

Recently, studies integrating transcriptome and proteome data have shown that correlation between mRNA and protein expression can be low due to a multitude of factors, including variability in the half-life of different RNA transcripts and in post-transcriptional machinery [41]. This lack of association could be largely based on factors that impact translational efficiency, mRNA-protein expression correlations, the physical properties of mRNA structure, codon bias, ribosomal density, higher inherent variability in mRNA expression, and the stability and abundance of mRNA molecules relative to proteins [41]. However, while transcriptomic and proteomic data often do not directly overlap, they may share a similar functional context, such as biological pathways or processes that are overrepresented during physiological responses [42]. Thus, a joint approach of transcriptomics and proteomics can provide information about associations between gene and protein expression that may not be detected when used separately.

In the studies presented in this thesis, I used transcriptomics and proteomics to discover the underlying molecular mechanisms that mediate physiological responses to stress in a free-ranging marine mammal, the northern elephant seal. I identified changes in gene and protein expression in response to single and repeated physiological stressors. Findings from these studies – alterations in expression of genes, their protein products, and the metabolic pathways that they regulate – provide information on the physiological impacts of stress and targeted biomarkers for assessing stress levels in vulnerable or endangered marine mammal populations.

Overall Objective

The objective of this study was to evaluate downstream mechanisms by which single (acute) and repeated (chronic) HPA axis activation may impact metabolic homeostasis and other aspects of physiology in a well-studied marine mammal, the northern elephant seal. To do this,

we simulated repeated physiological stress exposure by administering ACTH to juvenile elephant seals once daily for 4 days, inducing significant elevation in corticosteroid levels that we described in a previous publication [1]. However, the magnitude of elevation in cortisol, the corticosteroid most commonly used to evaluate stress in mammals, did not differ significantly in between the first and fourth ACTH response [1]. To understand the effects of changes in circulating corticosteroid levels on target tissues (e.g., blubber), we measured gene and protein expression levels in tissues collected from seals at different time points during the experiment. We compared transcriptome responses of elephant seal blubber tissue to the first and last ACTH administration by RNA sequencing (RNAseq). Further, to evaluate the functional consequences of changes in transcript expression, we compared proteome responses of blubber tissue to the first and last ACTH administration by liquid chromatography and tandem mass spectrometry (LC-MS/MS).

Chapter 2: Blubber Transcriptome Responses to Repeated ACTH Administration in a Marine Mammal

Introduction

Study objective. In this study, we evaluated the effects of repeated HPA axis activation on blubber gene expression in a fasting-adapted marine mammal, the northern elephant seal (*Mirounga angustirostris*). Elephant seals are an established marine mammal study system in which variation in baseline hormone levels [27], responses to acute ACTH administration [14, 25, 28, 29], and metabolic adjustments during fasting [30, 31] have been described. In addition, anesthesia procedures have been shown to minimize handling stress in this species, enabling measurements of true baseline hormone and gene expression levels [25]. Repeated physiological stress exposure was simulated in juvenile northern elephant seals by administering ACTH once daily for 4 days. Significant elevations in corticosteroid levels in response to ACTH have been reported in a previous publication [1]. To evaluate downstream mechanisms by which repeated HPA axis activation may impact metabolic homeostasis, we compared transcriptome responses of elephant seal blubber tissue to the first and last ACTH administration by RNA sequencing (RNAseq). We identified 27 genes that were differentially expressed in blubber during the response to the fourth versus the first ACTH challenge, many of which were associated with lipid storage and mobilization. These genes are potential biomarkers for discriminating between acute and repeated ACTH responses in marine mammals, which otherwise cannot be distinguished by cortisol profiles alone.

Methods

Experimental design. Juvenile (0.8-year old) northern elephant seals (*Mirounga angustirostris*) were sampled at Año Nuevo State Reserve (San Mateo County, CA) in Aug.–Nov. 2016. Repeated stress was simulated by administering ACTH to each study animal once every 24 hours for 4 consecutive days. Blood and blubber samples were collected before ACTH administration ("pre-ACTH") and 4 hours after ACTH administration ("ACTH response") on the first and fourth days (Fig. 2.1).

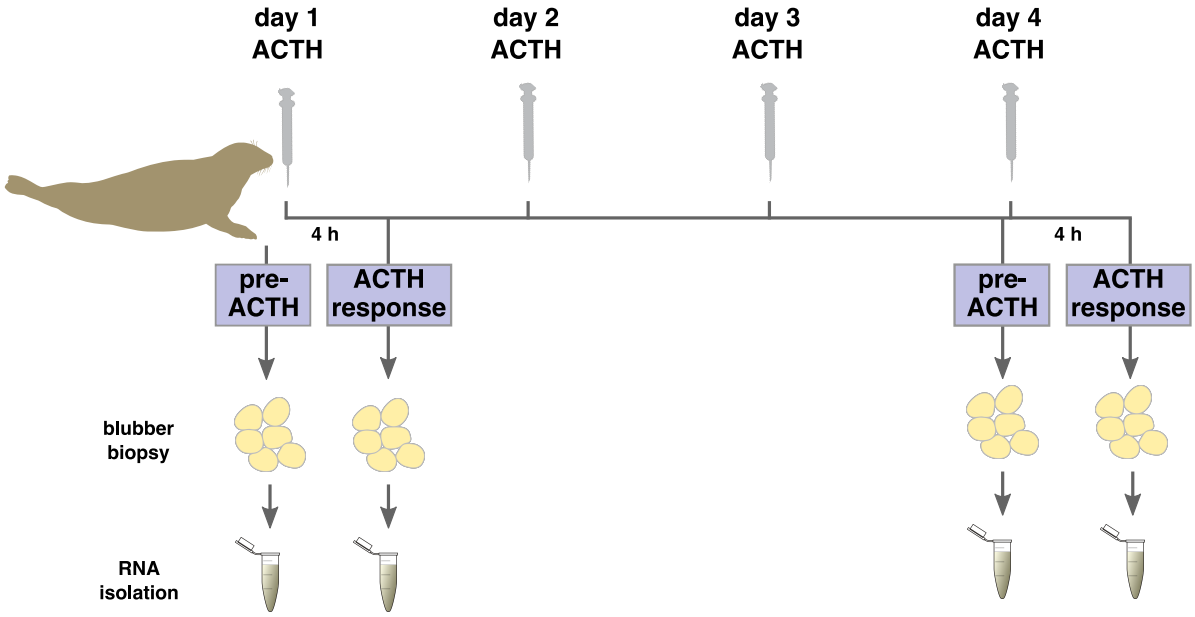

Figure 2.1. Repeated ACTH administration experiment (described in McCormley et al. [1]) and blubber tissue sampling design. ACTH was administered to juvenile elephant seals once every 24 hours for 4 days. Blubber biopsies were collected immediately before ACTH administration ("pre-ACTH") and 4 hours after ACTH administration ("ACTH response") on the first and fourth days. RNA isolated from blubber tissue was used for transcriptome sequencing. Seal (color modified, from https://pixabay.com), syringe (from https://pixabay.com), adipose (enhanced contrast, from https://openclipart.org), and microcentrifuge tube (from http://www.clker.com) images were obtained under CC0 1.0 Universal: CC0 1.0 Public Domain Dedication. License: https://creativecommons.org/publicdomain/zero/1.0.

Details of the experimental manipulation and hormone response have been reported previously [1]. Four of the 7 animals that participated in the repeated ACTH administration experiment described in McCormley et al. [1] (seals 2, 4, 6, and 7) were selected for the current study based on amounts of sequencing quality RNA that could be obtained from blubber samples.

Study subjects. All animal handling protocols were approved by Sonoma State University and University of the Pacific Institutional Animal Care and Use Committees (IACUC), Department of the Navy Bureau of Medicine and Surgery (BUMED), and were conducted under National Oceanic and Atmospheric Administration (NOAA) Fisheries Permit No. 19108. All procedures involving animals were conducted in accordance with the relevant guidelines and regulations of IACUC and BUMED protocols and the NOAA permit. Juvenile northern elephant seals have an additional haul out in the Fall and can be reliably found over multiple days at the rookery. In this study, juveniles (0.8-year old) were selected as they do not undergo biological stressors that adults are subjected to, such as molting, breeding, lactation, and reproduction, providing a natural level of corticosteroids prior to physiological manipulation to simulate the stress response [27, 43]. The study subjects, two females and five males, were selected based on size and body condition. All animals were healthy for their age, ranging from 99-137kg in mass, which permitted similar mass-specific doses of ACTH (Table 2.1). Seal mass was calculated by suspending animals from a tripod and scale (MSI tension dynamometer, Seattle, WA, USA). In addition, seals were marked for identification purposes using rear flipper tags (Dalton, Oxon, UK). All study animals remained at the rookery after the physiological manipulation and sample collection on each day.

Table 2.1. Experimental data for juvenile elephant seals used in the RNAseq study, including cortisol and aldosterone concentrations measured immediately before and 4 hours following administration of ACTH (pre-ACTH and ACTH response), respectively (from [1]). Aldosterone responses to the fourth ACTH challenge were significantly enhanced relative to the first ($p < 0.05$), while cortisol responses to the first and fourth ACTH administrations did not vary in magnitude [1].

Subject	**Sex**	**Mass (kg)**	**ACTH (U/kg)**	**Day**	**pre-ACTH cortisol (nM)**	**ACTH response cortisol (nM)**	**pre-ACTH aldosterone (pM)**	**ACTH response aldosterone (pM)**
Seal 2	M	119	0.17	1	198.7	760.2	812.6	1465.8
				4	202.2	2626.1	1204.2	2110.5
Seal 4	M	125	0.16	1	429.1	1298.5	828.4	2000.1
				4	227.7	1704.1	1476.5	2608.5
Seal 6	F	103	0.19	1	357.9	1542.1	670.9	1251.1
				4	494.3	4454.3	1610.1	2747.1
Seal 7	F	99	0.20	1	394.6	2598.6	792.2	1415.0
				4	355.5	2319.2	1291.3	2123.0

ACTH: adrenocorticotropic hormone.

Sedation, sample collection, and ACTH administration. Study animals were chemically immobilized and blood samples were collected as previously described [1]. Blubber samples ("day 1 pre-ACTH") were collected from the posterior flank region of each animal using a 6.0 mm diameter biopsy punch (Miltex, USA). The inner half (closest to musculature) of each biopsy sample was isolated, minced, and placed in cryovials containing RNA*later*™ Stabilization Solution (1.5 mL per ~300 mg tissue; Invitrogen, USA). Samples were incubated for 24 hours at 4°C, after which RNA*later*™ solution was removed and samples were stored at -80°C until RNA isolation. After baseline sampling, animals received 20 U of corticotropin LA gel (Wedgewood Pharmacy, Swedesboro, NJ, USA) via intramuscular injection (mass specific dose: 0.17 ± 0.02 U/kg). A paired set of blubber and blood samples was collected 4 hours after

ACTH administration ("day 1 ACTH response"); biopsies were collected from the contralateral side of the animal to the ACTH injection. On the second and third days of the experiment, ACTH was administered approximately 24 hours after the injection from the previous day, but no post-ACTH sampling was conducted. On the fourth day, pre-ACTH sampling ("day 4 pre-ACTH"), ACTH administration, and post-ACTH sampling ("day 4 ACTH response") were conducted as described for the first day.

Sample preparation

RNA isolation. Blubber samples were homogenized by bead beating in Qiazol (Qiagen, USA; ~100 mg tissue per 0.5 mL) using Bullet Blender Storm 24 (Next Advance, USA; Speed 12, two 2-minute cycles). After bead beating, another 0.5 mL of Qiazol was added to each sample and incubated for 5 minutes at room temperature with occasional vortexing. Lysates were further disrupted using QiaShredder tubes (Qiagen, USA) to shear genomic DNA and centrifuged for 15 minutes to separate lipids and cellular components. RNA was isolated from homogenates using the Lipid RNeasy Tissue Kit (Qiagen, USA) after chloroform (VWR Life Sciences, USA) phase extraction according to manufacturer's protocol. Genomic DNA was removed using a 20-minute on-column DNase I digest (Qiagen, USA). RNA concentration was quantified using Qubit 3.0 Fluorometer Broad Range RNA Assay (Life Technologies, USA). RNA integrity was evaluated using the Total RNA 6000 Pico kit on the 2100 Bioanalyzer (Agilent Technologies, USA). Mean (± SD) RNA integrity number (RIN) and 28S/18S rRNA abundance ratios were 6.81 ± 0.32 and 1.03 ± 0.27, respectively. We used Qiagen RNA*later*™ for preservation of blubber samples and isolation of RNA with RIN ≥ 7 in a previous study [14]. However, Ambion RNA*later*™ reagent used in this study did not adequately prevent RNA degradation. Due to the logistical challenges of the experiment, blubber sampling could not be

repeated and we proceeded with RNA sequencing, using ribosomal RNA depletion instead of polyA mRNA enrichment during library preparation to reduce 3' degradation bias [44]. Adequate amounts sequencing-quality RNA were obtained from 14 samples: the entire sample set (day 1 pre-ACTH, day 1 ACTH response, day 4 pre-ACTH, day 4 ACTH response) from seals 4, 6 and 7, and two samples (day 1 ACTH response, day 4 ACTH response) from seal 2.

RNA sequencing.

Library preparation and RNA sequencing. cDNA library preparation and Illumina HiSeq 4000 sequencing were conducted at the University of California, Berkeley QB3 Vincent J. Coates Genomics Sequencing Laboratory. Ribosomal RNA (rRNA) was depleted using Ribo-Zero rRNA Removal Kit (Human/Mouse/Rat; Illumina, Inc., USA). Yield and quality of mRNA were assessed using fluorometric methods and an Agilent 2100 Bioanalyzer, respectively (Agilent Technologies, USA). PrepX directional RNAseq library kits (WaferGen Bio-systems Inc., USA) were used for library preparation and libraries were quantified with KAPA Library Quantification kits for Illumina platforms (Kapa Biosystems, USA) using a Bio-Rad CFX Connect (Bio-Rad Laboratories, USA). Thirteen cycles of indexing PCR using KAPA High Fidelity Hotstart Amplification Kits (Kapa Biosystems, USA) were used before library quantification and validation. Individual libraries were barcoded, indexed as TruSeq single index per library, pooled in equimolar concentrations (400 ng), and sequenced as 100 base-pair paired-end reads on the Illumina HiSeq 4000. This generated a total of 150,055 sequenced megabases and a mean (± SD) of 26.9 ± 4.2 million paired-end 100-bp reads per sample. Sequencing data were demultiplexed and converted from bclfile to fastq file with Illumina's bcl2Fastq software v2.18 (Illumina, USA). Raw data were uploaded to NCBI Sequence Read Archive (SRA accession: SRP157071).

Computational assembly and analyses.

Methods development using eel pond mRNAseq protocol. To find the best transcriptome assembly, many different iterations of the computational analysis pipeline were attempted before selecting the final analysis. The Eel Pond mRNAseq computational analysis protocol v0.8.4 (https://readthedocs.org/projects/khmer-protocols/) was performed using JetStream cloud computing through XSEDE [45]. With this protocol, a few different parameters are implemented, such as the data trimming software, Trimmomatic, which is used for quality trimming on raw data generated by next-generation sequencing. Here, the sliding window was set to 4:2 instead of 4:5 in default parameters. Leading and trailing were also set to 2 instead of 5. Single end reads that were not aligned to a paired-end read were saved and combined into a single file. Paired-end reads were interleaved (combined) giving one final read file per sample. Trimmed and interleaved reads were subjected to digital normalization using diginorm, which normalized reads by median counts, removing abundant transcript isoforms that might create a bias for transcriptome assembly. Additionally, this helps by trimming off low abundance parts errors in reads of high coverage reads, which might be imputed as an isoform during assembly. By doing this, false positives can be removed and filtering by khmer size (all the possible subsequences of length k from a read) can be executed. After normalization, output files were used in de-novo transcriptome assembly without a reference genome to align to using Trinity (Haas et al., 2013) and differential gene expression analyses can be performed. We determined that using default settings under the Trinity v2.4.0 settings (https://github.com/trinityrnaseq/trinityrnaseq/wiki) produced a better-quality transcriptome, thus

we did all subsequent analyses following default settings that are well supported in transcriptomics literature.

De-novo transcriptome assembly. All computational analyses were conducted using the Extreme Science and Engineering Discovery Environment (XSEDE) Bridges Large High-Performance Computing Cluster [45] the Pittsburg Supercomputing Center through allocation TG-IBN150010. Transcriptome assembly was conducted using Trinity v2.4.0 [46]. Sequencing adapters and poor-quality bases were trimmed from reads using Trimmomatic run in Trinity with default settings. Quality of raw and trimmed reads was evaluated using FastQC v0.11.3 [47]. De novo assembly was conducted after in silico read normalization (50X coverage, kmer size 25 bp) using Trinity with all default settings (paired-end, strand-specific FR mode). Read mapping metrics were obtained using Bowtie2 v2.2.7 [48] and transcriptome completeness was analyzed using BUSCO v1.22 [49] (metazoan BUSCO dataset downloaded on 8/24/2017).

Transcriptome annotation. The assembly was annotated by aligning translated DNA query sequences against the UniProtKB/SwissProt protein sequence database (downloaded on 9/29/2017; "BLASTX") using DIAMOND v.0.8.31 [50] with e-value threshold for significant matches of 1e-3 and the --more-sensitive option. Putative protein sequences encoded in the transcriptome were predicted using TransDecoder v3.0.1 [51] and annotated against the UniProtKB/SwissProt protein sequence database ("BLASTP") using DIAMOND with e-value cutoff of 1e-3. Differentially expressed genes that did not have hits to the SwissProt database were manually annotated against the NCBI RefSeq database using NCBI BLASTX v2.7.1 with an e-value cutoff of 1e-5. Functional annotation of KEGG categories and GO enrichment was performed using DAVID Bioinformatics Resources v6.8 [52] with the human genome as background. Categories were considered significantly enriched at $p < 0.05$ (adjusted for multiple

comparisons using Benjamini-Hochberg correction [53]).

Gene expression analyses. All gene expression analyses were conducted using the Trinity pipeline. Transcript abundance was estimated using Kallisto v0.43.0 [54]. Differential expression analysis was performed at the gene level using the DESeq2 package in Bioconductor v3.5 [55] in R v3.4.1 with false discovery rate cutoff of 0.05 and log2 fold-change cutoff of 1.0. Pairwise comparisons between sampling conditions are shown in Table 3. Libraries from seal 2 were included only in the ACTH response comparison (day 4 ACTH response vs day 1 ACTH response). All other comparisons were conducted using libraries from seals 4, 6, and 7 only. Protein-protein interaction network prediction was conducted using STRING v10.5 [56]. Network data were imported into Cytoscape v3.5.0 [57] and filtered by experimental interactions using the edge weighted spring embedded layout. Unconnected nodes were removed from the analysis. Cytoskape network statistics were calculated using the network analyzer tool with an undirected analysis.

Results

Blubber transcriptome assembly. Blubber biopsies were collected from 4 juvenile northern elephant seals immediately prior to ("pre-ACTH") and 4 hours following ACTH administration ("ACTH response") on the first and fourth days of the experiment (Fig.1). Morphometric data, ACTH doses, and corticosteroid concentrations measured at the four sampling points are presented in Table 1 (from [1]). Fourteen cDNA libraries from day 1 pre-ACTH (seals 4, 6, and 7), day 1 ACTH response (seals 2, 4, 6, and 7), day 4 pre-ACTH (seals 4, 6, and 7), and day 4 ACTH response (seals 2, 4, 6, and 7) were sequenced using two Illumina HiSeq 4000 lanes. The libraries from seal 2 were used for assembly but were included only in the ACTH response comparison to increase power for detection of differentially expressed genes

(see Methods). Raw sequencing reads were uploaded to NCBI Short Read Archive (BioProject ID: PRJNA485363, SRA accession: SRP157071). A single reference transcriptome was assembled de novo using Trinity software. We assembled 1.36 billion bases into 2,031,456 contigs (or "transcripts") in 1,216,779 gene clusters (Table 2). The high number of transcripts is common for de novo assemblies [58] and is likely a result of sequence polymorphism, alternative splicing, and variability in individuals' responses to ACTH. The transcriptome assembly is available at figshare: (https://figshare.com/s/37cba07b2e9877f25b50).

To evaluate read representation in the reference transcriptome, we mapped sequenced reads back to the assembly. Ninety-two percent of reads mapped back as proper pairs to the assembly, suggesting that it accurately represents sequenced reads (Table 2).

Table 2.2. Transcriptome assembly metrics.

Metric	**Value**
Mean (± SD) reads per sample	26.9 ± 4.2 million
Assembled bases	1,361,692,561
Assembled contigs (transcripts)	2,031,456
Assembled transcript families	1,216,779
Annotated transcripts	372,783
Mean transcript length	670.3 bp
Read mapping rate	92.40%
Complete metazoan BUSCOs	85.8%
Complete and single-copy metazoan BUSCOs	51.6%
Complete and duplicated metazoan BUSCOs	34.1%
Fragmented metazoan BUSCOs	13.8%
Missing metazoan BUSCOs	0.4%

BUSCOs: Benchmarking Universal Single-Copy Orthologs. Read mapping rate: percent of sequenced reads mapping as proper pairs to the assembly.

To evaluate assembly completeness, we performed a search for metazoan Benchmarking Universal Single-Copy Orthologs (BUSCOs). Out of 978 metazoan BUSCOs in the OrthoDB catalog, 85.8% were present as complete orthologs in the seal assembly, 51.6% had matches to a single seal transcript, 34.1% were duplicated, 13.8% were fragmented, and only 0.4% were missing from the assembly (Table 2). This suggests that the blubber assembly is fairly complete as it contains the majority of orthologs predicted to be expressed in all metazoans. Due to the large number of short and potentially redundant transcripts in the assembly, we filtered the transcriptome using Transdecoder to retain only transcripts with putative protein-coding regions. The in silico-translated proteome contained 266,916 predicted proteins, some of which were predicted from multiple open reading frames of the same transcripts.

The reference transcriptome produced using the Eel Pond mRNAseq protocol produced 625,570,801 transcripts, compared to 1,361,692,561 transcripts assembled using Trinity default protocol. A common quality assessment of transcriptome assembly is the average contig (transcript) length (N50) [59]. The N50 for Eel Pond based assembly was 519 bp, compared to 670.3 bp using Trinity default protocol. This suggests that assembled transcripts were shorter in the assembly produced using the Eel Pond protocol, leading to fewer overlaps between reads, and resulting in shorter contigs. Shorter contigs also provide less power to detect differentially expressed genes [60]. Ninety-two percent of reads were mapped back as proper pairs to the assembly produced using the Eel Pond protocol, similar to the assembly produced using default Trinity protocol. Eel Pond transcriptome completeness was evaluated using BUSCO. Out of 978 metazoan BUSCOs, 80.5% were present as complete orthologs in the assembly, 47.1% had matches to a single transcript, 33.3% were duplicated, 18.5% were fragmented, and 1.0% were

missing from the assembly. These data suggest that the transcriptome assembly produced using the Eel Pond protocol was lower in quality than the transcriptome produced by Trinity default protocol. Therefore, we used the latter transcriptome assembly for all downstream analyses.

Transcriptome annotation. To identify seal homologs of vertebrate genes with known functions, the raw transcriptome assembly was annotated by translated nucleotide search (BLASTX) and the Transdecoder-predicted peptides were annotated by protein search (BLASTP) against the UniProt SwissProt protein database (e-value threshold 1e-3). BLASTX homologs were detected for 372,783 elephant seal transcripts and BLASTP homologs were detected for 164,557 Transdecoder-predicted elephant seal proteins. Transcriptome annotation data are available at figshare (https://figshare.com/s/37cba07b2e9877f25b50). To identify gene functional categories overrepresented in the blubber transcriptome, we used the DAVID functional annotation tool. Fifty-two metabolic (KEGG) pathways were enriched in the assembly relative to the human genome background (adjusted $p < 0.05$). The largest category was metabolic pathways, which contained 882 elephant seal homologs. Other pathways of interest included the child categories purine metabolism (135 genes), insulin signaling pathway (112 genes), Wnt signaling pathway (102 genes), AMPK signaling pathway (101 genes), insulin resistance (96 genes), thyroid hormone signaling pathway (94 genes), carbon metabolism (91 genes), adipocytokine signaling pathway (58 genes), fatty acid metabolism (44 genes), and fatty acid degradation (39 genes), among others. These KEGG enrichment data were similar to those from other elephant seal blubber transcriptomes [14, 61].

Differential gene expression. Differences in transcript abundance between sampling conditions were identified using DESeq2. The numbers of differentially expressed (DEG) and

annotated genes (adjusted p-value < 0.05 and FDR < 0.05) identified in each pairwise comparison between conditions are shown in Table 2.3.

Table 2.3. Number of DEGs identified in each pairwise comparison using DESeq2.

Comparison name	Pairwise comparison	total DEGs	upreg. DEGs	downreg. DEGs	annotated unique DEGs
First ACTH response	Day 1 ACTH response / Day 1 pre-ACTH	315	302	13	61
Fourth ACTH response	Day 4 ACTH response / Day 4 pre-ACTH	29	21	8	12
Overall ACTH response	Day 4 ACTH response / Day 1 pre-ACTH	624	479	145	99
Pre-ACTH comparison	Day 4 pre-ACTH / Day 1 pre-ACTH	66	39	27	24
ACTH response comparison	Day 4 ACTH response / Day 1 ACTH response	27	23	4	12

DEGs: differentially expressed genes. Annotated unique DEGs: elephant seal homologs of vertebrate proteins with known function, with multiple transcript isoforms collapsed to a single gene.

The magnitude and significance of gene expression differences in each comparison are presented in Figures 2.2 and 2.3. We first examined changes in gene expression in response to the first ACTH administration, fourth ACTH administration, and over the course of the entire experiment (day 1 pre-ACTH vs. day 4 ACTH response; "overall ACTH response;" Fig. 2.2).

We then compared expression between day 1 and day 4 pre-ACTH conditions ("pre-ACTH comparison") and between day 1 and day 4 ACTH responses ("ACTH response comparison," Fig. 2.3).

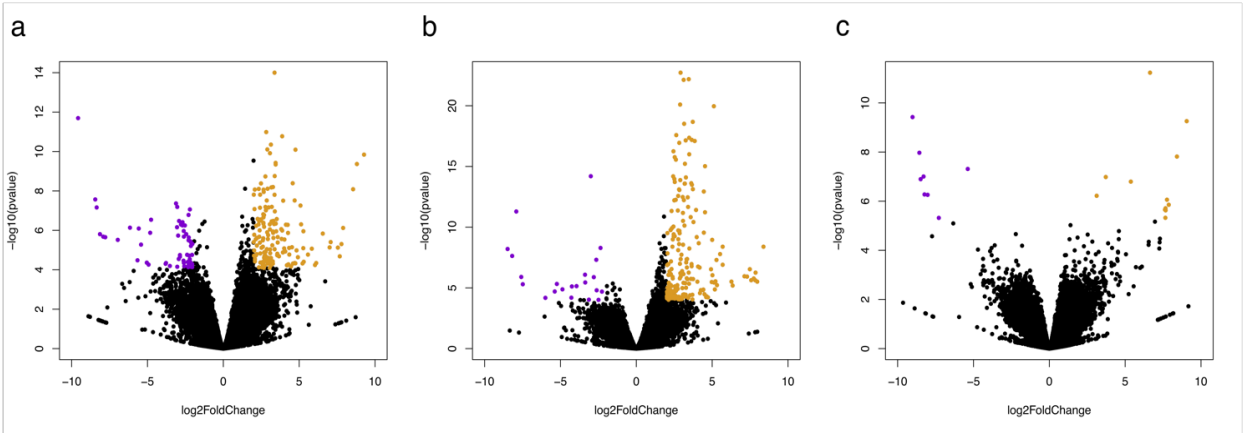

Figure 2.2. Volcano plots showing log2 fold change (x-axis) and significance (-log10 * adjusted p-value; y-axis) of genes differentially expressed during the overall ACTH response (a), first ACTH response (b), and fourth ACTH response (c). Significantly upregulated and downregulated genes are shown in orange and purple, respectively. Log2 fold-change and significance cutoffs for differential expression were |1| and 0.05, respectively.

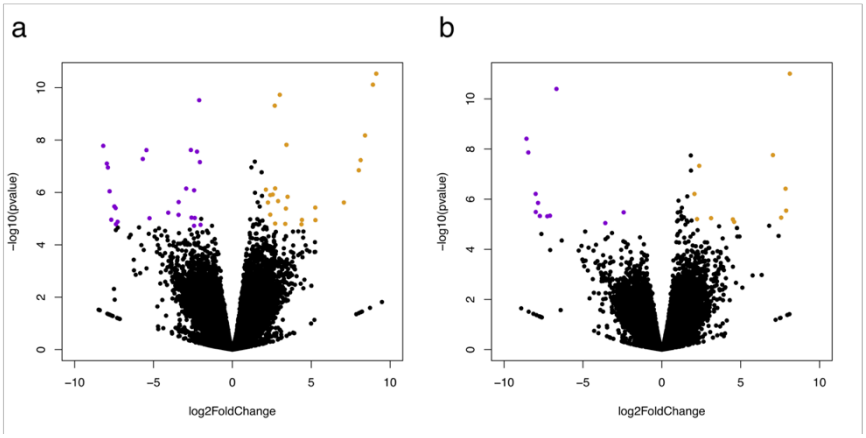

Figure 2.3. Volcano plots showing log2 fold change (x-axis) and significance (-log10 * adjusted p-value; y-axis) of genes differentially expressed in the pre-ACTH (a) and ACTH response (b) comparisons. Significantly upregulated and downregulated genes are shown in orange and purple, respectively. Log2 fold-change and significance cutoffs for differential expression were |1| and 0.05, respectively.

We identified 61 annotated, unique (i.e. all transcript isoforms collapsed into a single gene)

DEGs in response to the first ACTH administration, 12 DEGs in response to the fourth ACTH

administration, 99 DEGs in the overall ACTH response, 24 DEGs in the pre-ACTH comparison (Table 2.4) and 12 DEGs in the ACTH response comparison (Table 2.5).

Table 2.4. Genes differentially expressed in the pre-ACTH comparison (between pre-ACTH samples from day 1 and pre-ACTH samples from day 4).

Transcript	Log2 FC	Uniprot or NCBI Accession	Gene Name	Pathway/Process
TRINITY_DN590927_c3_g12	8.41	GCNT7_PIG	Beta-1,3-galactosyl-O-glycosyl-glycoprotein beta-1,6-N-acetylglucosaminyltransferase 7 (GCNT7)	protein glycosylation
TRINITY_DN560952_c14_g1	5.27	XP_020935075.1	6-phosphofructo-2-kinase/fructose-2,6-bisphosphatase 1 isoform X1 [Sus scrofa] (PFKFB1)	glycolysis and gluconeogenesis, response to GCs
TRINITY_DN566526_c4_g1	3.00	XM_008712174.1	PREDICTED: Ursus maritimus THAP domain containing 8 (THAP8), transcript variant X2, mRNA (THAP8)	transcription factor
TRINITY_DN590504_c4_g4	2.90	ACSM1_BOVIN	Acyl-coenzyme A synthetase ACSM1, mitochondrial precursor (ACSM1)	fatty acid activation and metabolism
TRINITY_DN560507_c9_g1	2.69	HMCS2_HUMAN	Hydroxymethylglutaryl-CoA synthase, mitochondrial precursor (HMGCS2)	ketogenesis
TRINITY_DN592323_c1_g1	2.41	TGO1_BOVIN	Transport and Golgi organization protein 1 homolog precursor (MIA3)	vesicular transport, collagen secretion
TRINITY_DN578525_c2_g2	2.13	209L2_MACMU	CD209 antigen-like protein 2 (CD209L2)	immune response
TRINITY_DN568360_c2_g1	1.91	KCRU_HUMAN	Creatine kinase U-type, mitochondrial precursor (CKMT1A)	phosphocreatine synthesis
TRINITY_DN591927_c4_g2	1.43	XM_006736873.1	cysteine dioxygenase type 1 (CDO1)	adipogenesis, taurine biosynthesis, cysteine degradation
TRINITY_DN571555_c4_g2	1.42	GPX3_RAT	Glutathione peroxidase 3 precursor (GPX3)	antioxidant response
TRINITY_DN572974_c28_g1	1.33	XM_021692420.1	adiponectin, C1Q and collagen domain containing (ADIPOQ)	fatty acid oxidation, insulin sensitivity
TRINITY_DN566880_c2_g2	1.20	HUTH_BOVIN	Histidine ammonia-lyase (HAL)	amino acid degradation

TRINITY_DN592891_c7_g1	1.13	MGST1_PIG	Microsomal glutathione S-transferase 1 (MGST1)	antioxidant response
TRINITY_DN575636_c4_g1	-1.30	ZBT46_MOUSE	Zinc finger and BTB domain-containing protein 46 (Zbtb46)	transcriptional repression, immune cell development
TRINITY_DN576776_c0_g1	-2.02	ITA2_HUMAN	Integrin alpha-2 precursor (ITGA2)	ECM organization, cell-matrix adhesion
TRINITY_DN545745_c4_g5	-2.06	FMOD_HUMAN	Fibromodulin precursor (FMOD)	collagen fibril formation
TRINITY_DN57258_c0_g6	-2.42	HBA_ODORO	Hemoglobin subunit alpha (HBA)	oxygen transport

FC: fold change (day 4 pre-ACTH / day 1 pre-ACTH); adjusted $p < 0.05$.

Table 2.5**.** Genes differentially expressed in the ACTH response comparison (between ACTH response samples from day 1 and ACTH response samples from day 4).

Transcript ID	**Log2 FC**	**Uniprot or NCBI Accession**	**Gene Name**	**Pathway/Process**
TRINITY_DN551341_c9_g1	1.94	GLRA2_RAT	Glycine receptor subunit alpha-2 (GLRA2)	glycine receptor
TRINITY_DN570625_c1_g4	1.81	ATS16_HUMAN	A disintegrin and metalloproteinase with thrombospondin motifs 16 (ADAMTS16)	blood pressure regulation
TRINITY_DN587322_c7_g1	1.23	PIAS4_HUMAN	E3 SUMO-protein ligase PIAS4 (PIAS4)	protein sumoylation, cell stress response, metabolic homeostasis
TRINITY_DN592677_c7_g3	1.18	XM_022511147.1	Perilipin 1 (PLIN1)	lipolysis regulation, insulin sensitivity
TRINITY_DN549777_c0_g1	1.09	PLIN4_HUMAN	Perilipin-4 (PLIN4)	triacylglyceride packaging
TRINITY_DN587150_c2_g2	1.06	ZA2G_BOVIN	Zinc-alpha-2-glycoprotein (AZGP1)	lipid mobilization
TRINITY_DN591317_c4_g2	1.04	ACSL1_MOUSE	Long-chain-fatty-acid--CoA ligase 1 (ACSL1)	fatty acid catabolism, fatty acid synthesis
TRINITY_DN587426_c4_g1	1.02	CIDEA_MOUSE	Cell death activator CIDE-A (CIDEA)	lipolysis regulation, insulin sensitivity
TRINITY_DN591034_c2_g1	-1.96	BGH3_PIG	Transforming growth factor-beta-induced protein ig-h3 (TGFBI)	cell adhesion, adipogenesis
TRINITY_DN589692_c4_g2	-2.82	XM_002919434.3	PREDICTED: Ailuropoda melanoleuca C1q and tumor necrosis factor related protein 3, mRNA (C1QTNF3)	inhibition of gluconeogenesis and inflammation

FC: fold change (day 4 ACTH response / day 1 ACTH response); adjusted $p < 0.05$.

Several DEGs had hits to poorly characterized genomic regions of other mammals (first ACTH response: 31, fourth ACTH response: 7, overall ACTH response: 34, pre-ACTH comparison: 8, ACTH response comparison: 6), and thus could not provide functional insights. Functional annotation of DEG lists identified 2 Gene Ontology (GO) biological process categories enriched in first ACTH response (positive regulation of fat cell differentiation, negative regulation of transcription from RNA polymerase II promoter), 18 GO categories enriched in overall ACTH response (including fatty acid transport, long-chain fatty acid metabolic process, long-chain fatty acid-CoA ligase activity, positive regulation of fat cell differentiation, response to hypoxia, transcription factor binding) and 1 GO category enriched in the ACTH response comparison (zinc ion binding). KEGG categories were significantly enriched only in overall ACTH response dataset (ECM-receptor interaction, focal adhesion, pathways in cancer, and small cell lung cancer).

We next manually categorized unique annotated DEGs based on known function using literature search to understand their potential roles in repeated stress responses and metabolic homeostasis. Genes that were upregulated (n=58) during the first ACTH response included many known GC targets and genes of interest involved in oxidative stress defenses (GPX3), fatty acid oxidation (ACADM), immune function (TLR4), adipogenesis (DKK1), lipid and monocarboxylate transport (SLC16A9), ketogenesis (HMGCS2), insulin resistance and obesity (ZBTB16*),* NADP biosynthesis and saturated fatty acid metabolism (NADK2)*,* circadian rhythm (PER1), and inactive steroid receptor complexes (FKBP5). Other differentially expressed genes were associated with sphingolipid metabolism*,* DNA replication and repair, cytoskeleton and ECM remodeling, protein synthesis and posttranslational modification, protein transport, and embryonic development and cell differentiation. Genes downregulated (n=3) during the first

ACTH response were associated with ECM remodeling and insulin resistance (ADAMTS9), cell growth and migration (ABI2), and negative regulation of tyrosine kinase activity (PTPN12).

Genes upregulated (n=10) during the fourth ACTH response included those associated with protein degradation (CACYBP), inhibition of apoptosis (DYRK3), and transcriptional regulation (NCOR1), as well as those involved in cell adhesion and migration, sphingolipid biosynthesis, and nucleotide metabolism. Genes downregulated (n=2) during the fourth ACTH response included an activin receptor associated with adipogenesis (ACVR2A) and a protein glycosylation enzyme. Only two DEGs (ABI2 and SPTSSB) were common between day 1 and day 4 ACTH responses.

Genes of interest that were upregulated (n=75) during the overall ACTH response included those associated with lipolysis (CES1D), ketogenesis (HMGCS2), adipogenesis (DKK1), oxidative stress (FMO2), regulation of energy balance (LEP), fatty acid oxidation (ACSL1), fatty acid biosynthesis (ACSM1, ACSM4, SCD2, GPD1), lipid binding and transport (APOD, SLC27A6, ABCA6, ABCA10), steroid hormone transport (SLC10A6), sphingolipid metabolism (ACER2), and amino acid transport (SLC1A3). Upregulated genes also included an enzyme that links glycolytic and triglyceride synthesis pathways (GPD1), angiotensinogen (AGT) precursor, and a transcriptional activator that increases sensitivity to low GC concentrations (GMEB1). Genes of interest that were downregulated (n=24) over the course of the entire experiment included those associated with inflammation and insulin resistance (CD44), stress and hormone responses (DRG1), local production of triiodothyronine (DIO2), regulation of glycolysis (PFKFB1), gene transcription and adipocyte differentiation (JUNB), as well as those involved in ECM remodeling and cell adhesion.

Annotated genes upregulated (n=13) in the pre-ACTH comparison were associated with processes of interest including glycolysis (PFKFB1), ketogenesis (HMGCS2), fatty acid activation and metabolism (ACSM1), regulation of fatty acid oxidation and insulin sensitivity (ADIPOQ), adipogenesis (CDO1), protection from oxidative damage (GPX3, MGST1), immune response (CD209L2), and amino acid degradation (HAL). Other upregulated genes were associated with phosphocreatine synthesis, collagen secretion, gene transcription, and protein glycosylation. Genes downregulated (n=11) in the pre-ACTH comparison were associated with transcription (ZBTB46), suppression of inflammation (SETD6), oxidative stress protection (GDAP1) and transcriptional repression by nuclear receptors and inhibition of adipogenesis (NCOR1). Other downregulated genes were associated with ECM organization, cell adhesion, and motility, hematopoiesis and oxygen transport (Table 2.4).

Annotated genes that were upregulated (n=9) in the ACTH response comparison included those involved in lipid droplet formation (PLIN1, PLIN4, CIDEA), lipolysis (AZGP1), fatty acid metabolism (ACSL1), as well as cell adhesion and ECM remodeling, protein sumoylation, and glycine binding. Genes downregulated in the ACTH response comparison (n=3) included those involved in adipogenesis, adipokine signaling, and fatty acid uptake (THBS1), lipid oxidation (C1QTNF3), and cell adhesion (TGFBI) (Table 2.5).

Lastly, we examined the potential for interaction between proteins encoded by annotated DEGs by conducting protein-protein interaction (PPI) network analysis using the overall ACTH response dataset. The predicted PPI network contained 20 nodes, 25 edges, network density of 0.132, network heterogeneity of 0.687, network centralization of 0.263, average local clustering coefficient of 0.135, and PPI network enrichment p-value of 0.00386 (Fig. 2.4), suggesting that

DEGs are likely functioning as a coordinated network to regulate cellular and metabolic responses to repeated ACTH administration.

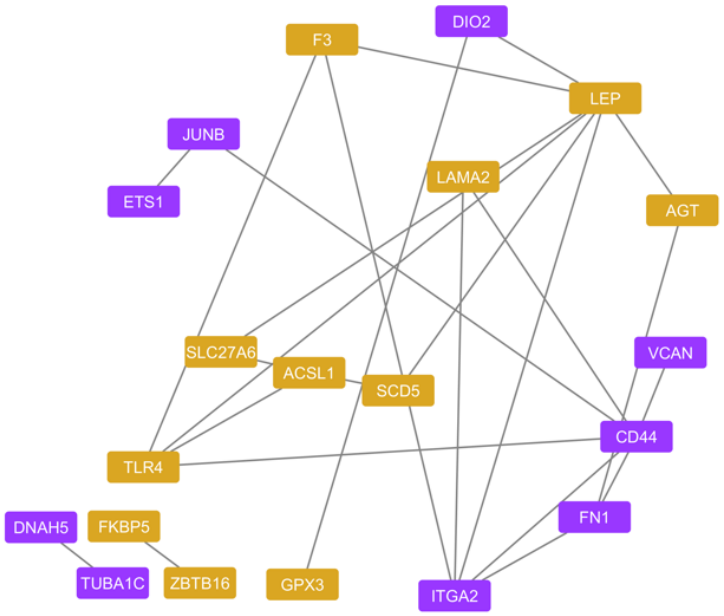

Figure 2.4. Predicted protein-protein interaction (PPI) network ($p<0.05$) for genes differentially expressed over the course of the experiment (overall ACTH response). Upregulated and downregulated genes are shown in orange and purple, respectively.

Discussion

Overall, this study shows that gene expression differences between single and repeated ACTH responses in marine mammal blubber are detectable despite similarities in cortisol levels, providing more sensitive indication of stress response states than endocrine profiles alone. We administered ACTH once daily for four days to juvenile northern elephant seals and previously reported significant elevation in corticosteroid levels in response to the first and fourth administrations [1]. However, while the aldosterone response was facilitated by repeated ACTH

administration, the cortisol response was not, highlighting the unreliability of glucocorticoid measurements alone for discriminating between acute and repeated HPA axis activation. Therefore, we used RNAseq to examine downstream changes in blubber gene expression in response to repeated ACTH administration. Such changes in blubber gene activity reflect activation of genomic and cell-surface hormone receptors, including glucocorticoid receptor (GR), mineralocorticoid receptor (MR), and the adrenocorticotrophic hormone receptor (MC2R) in multiple cell types, capturing the complexity of target tissue responses [62-64]. We identified DEGs during the responses to both the first and fourth ACTH administration, although the number of DEGs identified in response to the latter was much smaller than the former. We also identified transcriptional differences between pre-ACTH and post-ACTH response states from the first and fourth days. Annotated DEGs were associated with functions such as lipid and carbohydrate metabolism, adipogenesis, adipokine regulation of energy balance, insulin resistance, oxidative stress, transcriptional regulation, and ECM remodeling in other mammals and provide insights into mechanisms by which repeated HPA axis activation may affect marine mammal physiology.

Genes upregulated in response to the first ACTH challenge were associated with protection from oxidative damage, fatty acid oxidation, immune response, adipogenesis, nutrient transport, sphingolipid and ketone metabolism, cell differentiation, cytoskeletal and ECM remodeling, and insulin resistance and obesity in other animals, while downregulated genes were associated with ECM remodeling and cell migration. Several identified DEGs are primarily known for their roles in other biological processes (e.g. embryonic development) and have only recently been implicated in lipid metabolism and adipogenesis. These include GDF3 and DKK1, which promote adipogenesis and metabolic homeostasis [65, 66], and the transcriptional

regulator ZBTB16, which plays a role in obesity and brown adipose energetics [67]. This is consistent with pro-adipogenic effects of GCs in other mammals [24]. Other genes upregulated in response to the first ACTH administration included those associated with immune response, which is consistent with studies in other mammals in which acute stress enhanced immune capacity, while chronic stress had immunosuppressive effects [68]. DKK1 and similar functional classes of genes associated with adipogenesis, immune response, and extracellular matrix function were also upregulated in blubber 2 hours after a single ACTH administration [14]. This suggests that transcriptional changes measured 2 and 4 hours after ACTH administration are capturing the same biological response in blubber. Upregulation of genes involved in lipid metabolism is consistent with known lipolytic effects of corticosteroids and the increase in circulating free fatty acid levels that has been measured in response to ACTH in this species [25, 29, 69]. Interestingly, one upregulated gene, FKBP5, is a GR antagonist [70], suggesting a potential negative feedback mechanism to limit acute responses to ACTH. Genes downregulated in response to the first ACTH administration were associated with ECM remodeling and cell migration, suggesting suppression of some energy-intensive functions during the ACTH response. However, many upregulated genes were also involved in ECM remodeling, highlighting the complexity of this specialized connective tissue.

Genes upregulated in response to the fourth ACTH challenge included those associated with regulation of transcription, protein degradation, inhibition of apoptosis, and cell migration, while downregulated genes included those associated with adipogenesis and post-translational protein modification. Significantly fewer DEGs were identified in response to the fourth ACTH challenge compared to the first, potentially because many cellular responses were already engaged by the previous ACTH responses. Upregulated genes included two that may protect

blubber tissue from deleterious effects of repeated corticosteroid exposure: DYRK3, a kinase that phosphorylates and activates the sirtuin SIRT1 and promotes cell survival during stress [71] and NCOR1, a nuclear corepressor that mediates ligand-induced downregulation of the GR gene [72]. DYRK3 was also upregulated in response to a single ACTH administration in a previous study [14]. Surprisingly, the type II BMP receptor ACVR2A, which promotes adipogenesis by GDF6 signaling [52], was downregulated during the fourth ACTH response, whereas pro-adipogenic factors were upregulated in response to a single ACTH challenge in this and a previous study [14]. These results suggest that the transcriptional response to a fourth sequential ACTH administration may serve to promote cell survival and limit adipogenesis and GC sensitivity. However, it is unclear whether this potential negative feedback is sufficient to prevent deleterious consequences of repeated HPA axis activation, as there were dramatic gene expression differences between the baseline state on day 1 and the ACTH response state on day 4.

The largest number of DEGs was identified in the overall ACTH response comparison, as this comparison captured all gene expression differences between pre-ACTH samples on day 1 and post-ACTH samples on day 4. Upregulated genes of interest suggest that repeated ACTH administration impacted lipid and ketone metabolism, adipogenesis, redox homeostasis, and thyroid hormone signaling. Upregulation of genes encoding leptin and the ketogenesis enzyme HMGCS2 suggests potential increase in energy expenditure and ketone production to support metabolic demands of repeated HPA axis activation. However, leptin is also involved in modulating immune responses [73], and its role in elephant seal metabolism is currently unclear [74]. Genes associated with lipolysis and fatty acid oxidation were upregulated concomitant with those involved in fatty acid and triglyceride synthesis (e.g. ACSM1). ACSM1 was also

upregulated 24 hours after a single ACTH administration in a previous study [14]. Glucocorticoid-associated lipogenesis has been described in obese humans [24, 75], and may be mediated by MR [76]. Upregulation of GPD1, which promotes triglyceride synthesis in response to excess glucose, and AGT, a component of the renin-angiotensin (RAS) system associated with obesity, suggest that repeated ACTH administration may potentially increase lipogenesis in a naturally obese and insulin-resistant mammal [31]. Downregulation of the iodothyronine deiodinase DIO2, which converts thyroxine to bioactive triiodothyronine (T3), is consistent with suppression of circulating T3 levels after repeated ACTH administration in the same animals [1]. Therefore, these data suggest fasting-adapted mammals may simultaneously metabolize and maintain lipid stores during repeated HPA axis perturbation. However, suppression of T3 and increased lipogenesis may decrease energy expenditure and impair the ability of fasting-adapted marine mammals to participate in energetically demanding life history stages.

Our previous studies have shown that while cortisol levels returned to baseline within 24 hours of each ACTH administration [1], changes in gene expression in response to ACTH could be detected even when cortisol was no longer elevated [14]. To identify whether transcriptional changes alone can be used to detect repeated ACTH exposure, we compared gene expression profiles in blubber samples collected immediately prior to the first and fourth ACTH challenges. Genes upregulated in pre-ACTH samples from day 4 relative to day 1 were associated with regulation of glycolysis, ketogenesis, fatty acid biosynthesis, adipokine signaling, oxidative stress, and adipogenesis. Downregulated genes were associated with genetic and epigenetic regulation of transcription, mitochondrial dynamics, and immune cell differentiation. These results suggest that recovery from repeated ACTH administration may involve metabolic and cellular adjustments such as increased glycolysis and fatty acid oxidation, synthesis of fatty acids

and ketones, antioxidant responses, and increased adipogenesis. Upregulation of antioxidant enzymes GPX3 and MGST1 may serve to protect seal tissues from oxidative damage associated with exposure to GCs [77, 78]. Two genes upregulated in day 4 pre-ACTH samples (24 hours after the third ACTH challenge) – ACSM1 and CDO1 – were also upregulated 24 hours after a single ACTH administration in a previous study [14]. However, genes associated with ketogenesis and antioxidant defenses were not altered in response to a single ACTH challenge and may therefore serve as markers of recently experienced repeated HPA axis activation.

To identify transcriptional differences between blubber responses to single and repeated ACTH challenges, we compared the ACTH response samples from days 1 and 4. We identified nine DEGs that were upregulated and three that were downregulated in day 4 ACTH response samples compared to those from day 1, and suggest them as potential markers of repeated HPA axis stimulation in marine mammal blubber. Upregulated genes were associated with lipid droplet formation, energy homeostasis, and lipolysis, while downregulated genes were associated with adipogenesis and lipid uptake and oxidation. Three upregulated genes encoded the lipid droplet-associated proteins CIDEA and the perilipins PLIN1 and PLIN4, which are involved in regulation of lipolysis and lipid droplet expansion [79]. While GCs have been shown to upregulate some lipid droplet proteins [80, 81], they mainly affect perilipins by inhibitory phosphorylation that facilitates lipolysis [82]. Transcriptional upregulation of perilipins in response to repeated ACTH administration may function to restrict lipolysis in an attempt to conserve lipid stores in a fasting-adapted mammal. Other genes upregulated during the fourth ACTH response compared to the first included the glycoprotein AZGP1 and glycine receptor GLRA2, which promote lipolysis [83], ADAMTS16, which is associated with regulation of blood pressure [84], PIAS4, which inhibits AMPK and SIRT1 (and thus derepresses lipid and

protein synthesis [85, 86]), and CNTNAP3, a cell adhesion protein that is a marker of brown adipocytes [87]. Downregulated genes included THBS1, which is associated with adipocyte proliferation and fatty acid uptake [88], C1QTNF3, an adipokine that increases hepatic lipid oxidation and decreases lipid synthesis, gluconeogenesis and inflammation [89], and TGFBI, a TGF beta family member associated with type 2 diabetes and adipogenesis [90]. While interpretation of DEG roles in ACTH responses is complicated by their pleiotropic (or poorly described) functions and the heterogeneity of cell types in blubber tissue, these data suggest that repeated ACTH administration primarily increases lipid catabolism and dysregulates lipid storage. This is consistent with significant declines in circulating triglyceride levels detected after 4 ACTH challenges [91]. Therefore, repeated HPA axis activation may impact the ability of marine mammals to maintain prolonged fasts and high levels of energy expenditure required to participate in key life history stages. For example, depletion of energy reserves by repeated stress would impact reproductive expenditure (e.g. milk production, male-male competition), decreasing fitness [92].

To our knowledge, this study was the first to examine changes in gene expression in wild marine mammals in response to repeated ACTH administration. Despite the limitations of small sample size, high degree of individual variability in ACTH responses, and small number of ACTH challenges, we identified dozens of DEGs that were differentially expressed in response to repeated ACTH administration. Most significantly, we identified gene expression differences between single and repeated ACTH responses in blubber despite similarities in cortisol levels, providing more sensitive indication of response states than endocrine profiles alone. Further work is necessary to correlate transcriptional changes with metabolic and redox profiles and validate the ability of these biomarkers to discriminate baseline stress states in marine mammals.

Nevertheless, these findings provide some of the first insights into the physiological impacts of repeated ACTH administration in free-ranging marine mammals, and suggest potential molecular markers of repeated stress exposure that can complement other approaches used by conservation biologists to evaluate the effects of anthropogenic activity on threatened wildlife populations.

Chapter 3: Blubber Proteome Responses to Repeated ACTH Administration in a Marine Mammal

Introduction

Study objective. Analyzing changes in expression of downstream targets (genes, proteins) of hormones using omics approaches is an effective, comprehensive approach to understand the molecular consequences of the physiological stress response. Combining multiple non-targeted approaches can lead to a more complete understanding of cellular responses to stress and its impacts on metabolic homeostasis. In fasting-adapted marine mammals, lipids stored in modified adipose tissue (blubber) are used to fuel metabolic demands associated with natural life history challenges (e.g. molting, breeding, lactating). These lipid stores are also mobilized in response to additional unpredictable stressors [11, 24]. To gain insight into how metabolic processes in adipose tissue of marine mammals are altered in response to acute and repeated HPA axis activation, we collected blubber samples from juvenile northern elephant seals (*Mirounga angustirostris*) before and four hours after the first and fourth of ACTH doses administered once daily for four days. RNA and proteins were isolated simultaneously from the same blubber cells, and RNAseq was used to determine changes in gene expression in response to ACTH [93]. Proteomics was then used to explore changes in the abundance of metabolic and structural proteins in response to the same experiment. Implementation of both transcriptomics and proteomics addresses two different aspects of adipose biology: metabolic enzyme changes in response to physiological stress and extracellular matrix remodeling in the dynamic relationship with adipogenesis.

We identified 10 differentially expressed proteins in blubber in response to the fourth versus the first ACTH administration, which were associated with cell adhesion, ECM deposition and remodeling, and cytoskeleton dynamics. Interestingly, increased ECM remodeling has been

associated with adipogenesis [94], which is stimulated by GCs. This is supported by upregulation of gene transcripts associated with adipogenesis and downregulation of adipogenesis inhibitors in response to ACTH [93], highlighting the potential relationship between adipocyte differentiation and ECM deposition during stress. In addition, other differentially expressed proteins of interest can be used as biomarkers of stress due to their increased stability compared to RNA and function as downstream mediators of stress hormones, providing the ability to measure stress in vulnerable and endangered populations of marine mammals (e.g. cetaceans), from which tissue collection, handling, and preservation is logistically difficult.

Methods

Experimental design.

Study animals and experimental design. Juvenile (0.8-year old) northern elephant seals (*Mirounga angustirostris*) were sampled in Aug.-Nov. 2016 at Año Nuevo State Reserve (San Mateo County, CA) under handling protocols approved by Department of the Navy Bureau of Medicine and Surgery (BUMED), University of the Pacific and Sonoma State University Institutional Animal Care and Use Committees (IACUCs), and under National Oceanic and Atmospheric Administration Fisheries Permit No. 19108. Study animals received 20 U of ACTH once every 24 hours for 4 consecutive days to simulate repeated stress responses. Blood and blubber tissue samples were collected prior to ACTH administration ("pre-ACTH") and 4 hours after ACTH administration ("ACTH response") on the first and fourth days, as described previously [1]. Endocrine and blubber transcriptome responses of study animals to this manipulation have been described [1, 93] (Fig. 2.1). Two of the 7 animals that participated in

this experiment (seal 6 and seal 7), and for which transcriptome data are available *[93]*, were used in the current study.

ACTH administration and blubber sampling. Study animals were chemically immobilized and baseline blood and blubber samples ("day 1 pre-ACTH") were collected as previously described [1, 93]. Blubber samples were collected from the posterior flank region of each animal using a 6.0 mm diameter biopsy punch (Miltex, USA). The inner half (closest to musculature) of each biopsy was minced and incubated in RNA*later*™ Stabilization Solution (1.5 mL per ~300 mg tissue; Invitrogen, USA) for 24 hours at 4°C, after which the solution was removed, and samples were transferred to -80°C for storage. After baseline sampling, animals received an intramuscular injection of 20 U of corticotropin LA gel (Wedgewood Pharmacy, USA) and a paired set of blubber and blood samples was collected 4 hours after ACTH administration ("day 1 ACTH response"). On the second, third, and fourth days of the experiment, ACTH was administered approximately 24 hours after the injection from the previous day. Day 4 pre-ACTH sampling ("day 4 pre-ACTH"), ACTH administration, and post-ACTH sampling ("day 4 ACTH response") were conducted as described for the first day.

Sample preparation.

Protein isolation and processing. Protein isolation from blubber tissue was conducted as previously described [95]. Briefly, blubber samples were homogenized in Qiazol (Qiagen, USA) using Bullet Blender Storm 24 (Next Advance, USA; Speed 12, two 2-minute cycles) and QiaShredder tubes (Qiagen, USA). After removal of RNA using chloroform phase extraction, proteins were precipitated from the organic phase using isopropanol, washed with 0.3 M guanidine hydrochloride in 95% ethanol, and stored at -80°C in wash solution. Protein pellets were washed with ethanol, resuspended in Denaturing Buffer (1% w/v sodium deoxycholate

(SDC), 8 M urea, 5 mM DTT in 50 mM ammonium bicarbonate), denatured for 1 hour at 37°C, and alkylated with 15 mM iodoacetamide at room temperature for 30 minutes. Alkylation was quenched with 5 mM DTT. Samples were diluted to reduce urea concentration to < 2 M and digested in solution using Trypsin Gold ™ (Mass Spectrometry Grade, Promega, USA) at 1:50 µg enzyme to protein ratio. Samples were acidified to pH < 2 to precipitate SDC and desalted using Pierce C18 Spin Columns (Thermo Scientific, USA). Peptides were lyophilized and resuspended in 0.5 M triethylammonium bicarbonate (TEAB), and 30 µg of each sample was labeled using 30 µl of iTRAQ 8-plex reagents (SCIEX, USA) according to the manufacturer's protocol. Labeled samples were pooled and fractionated offline using Pierce High pH Reversed-Phase Peptide Fractionation Kit (Thermo Scientific, USA) according to the manufacturer's protocol, with one additional column wash (5% acetonitrile, 0.1% triethylamine in LC/MS-grade water). Fractions were pooled in pairs (fractions 1 and 5, 2 and 6, 3 and 7, and 4 and 8), lyophilized, and resuspended in 0.1% formic acid in LC/MS-grade water.

BCA assay. Protein or peptide concentration was estimated using the bicinchoninic acid (BCA) assay (Thermo Scientific, USA). Samples were assayed in duplicate (mean CV = 2.04%, SD=2.61) Prism7 (GraphPad, USA) was used to fit and extrapolate the standard curve (third-order polynomial fit, R^2=0.99) to obtain sample concentrations.

Peptide sequencing.

HPLC-MS/MS. Peptide samples were diluted to 150 ng/µl with 0.1% formic acid in LC/MS-grade water and 5 µl were loop injected by a Dionex Ultimate 3000 autosampler onto a reversed-phase trap column (Acclaim™ PepMap™ 100 C18 LC column; 75 µm i.d. x 2 cm, 3 µm particle size, 100 A pore size, Thermo Fisher Scientific, USA). Peptides were eluted onto a reversed-phase analytical column (EASY-Spray™ C18 LC column; 75 µm i.d. × 15 cm, 100 A,

Thermo Fisher Scientific, USA) held at 35°C for HPLC. Solvents A and B were 0.1% formic acid in water and in acetonitrile, respectively. Solvent B was used as following: 3% for 5 min, 3%–28% for 75 min, 28%–45% for 25 min, 45%–95% for 5 min, 95% for 5 min, return to 3% for 5 min, followed by 2% for 25 min. Flow rates were held at 300 nl/min with each sequencing run set to 140 minutes. Mass spectrometry analysis was performed using Orbitrap Fusion™ Tribrid™ mass spectrometer equipped with an EASY-Spray™ ion source (Thermo Fisher Scientific, USA) operated in a data dependent acquisition (DDA) manner by Xcalibur 4.0 software (Thermo Fisher Scientific, USA). Instrument and data acquisition settings were the same as previously reported [95], with the exception of the scan range (400-1600 da), MS1 orbitrap resolution (60,000), scan time (10-130 minutes), and HCD collision energy (33 ± 3%, stepped). MS1 spectra were resolved by the orbitrap; precursor ions selected using DDA were quadrupole filtered and fragmented using HCD. MS2 product ions with corresponding iTRAQ labels were also resolved by the orbitrap.

Data analysis.

Protein identification. MS/MS data analyses were performed using Proteome Discoverer 2.2.0.388 (Thermo Scientific, USA). Peptide spectra were searched against the entire UniProt SwissProt database (downloaded on 2/13/2018) using SEQUEST. In addition, spectra were searched against the common Repository of Adventitious Proteins (cRAP, https://www.thegpm.org/crap/index.html) to identify contaminants associated with sample preparation. Search parameters were the same as previously reported [95], with the exception of adding the iTRAQ label mass as a static modification (iTRAQ8plex / +304.205 Da (Any N-Terminus). False discovery rate (FDR) for peptide spectral matches (PSMs) and peptides were estimated by searching reversed decoy databases generated from the Uniprot SwissProt and

cRAP databases. Results were filtered to remove identified contaminants and retain peptides with target FDR < 1%. Proteins were considered "unique" if they had 2 or more unique peptides that mapped back to the spectra. DAVID Bioinformatics Resources v6.8 [96] server was used to identify KEGG and GO categories that were overrepresented in the elephant seal blubber proteome relative to the entire human proteome (Benjamini-Hochberg adjusted [53] $p \leq 0.05$)

Protein quantification. Protein quantification was conducted using Proteome Discoverer 2.2.0.388 (Thermo Scientific, USA). MS/MS data were filtered to retain only proteins that had 2 or more unique peptide hits and were identified in all 8 samples with high confidence (FDR <1%). Quantitative abundances were normalized and scaled to the same total peptide amount per iTRAQ channel, so that the average abundance per protein and peptide was 100. The co-isolation threshold was set to 50 to reduce isolation interference with label quantification. Ratio calculations were summed abundance values. ANOVA was used to determine whether protein abundances significantly differed between samples. Biological replicates were grouped by condition, normalized, and scaled. Ratio abundances were calculated for the following sample comparisons: day 4 ACTH response vs day 1 pre-ACTH ("overall response"), day 1 ACTH response vs day 1 pre-ACTH ("first ACTH response"), day 4 ACTH response vs day 4 pre-ACTH ("fourth ACTH response"), day 4 pre-ACTH vs day 1 pre-ACTH ("pre-ACTH comparison"), and day 4 ACTH response vs day 1 ACTH response ("ACTH response comparison"). Proteins that had ratio abundance above 1.2 or below 0.8 between conditions (as recommended in the literature [97-101]) and $p < 0.05$ were considered differentially expressed.

Results

In this study, we characterized the blubber proteome responses of juvenile northern elephant seals to repeated ACTH administration. Blubber biopsies were collected from 2 elephant seals (seal 6 and seal 7) immediately prior to ("pre-ACTH") and 4 hours following ACTH administration ("ACTH response") on the first and fourth days of the experiment (Fig. 2.1). The animals' endocrine and blubber transcriptome responses to repeated ACTH administration have been reported previously [1, 93]. Specifically, seals 6 and 7 exhibited the largest (in magnitude) corticosteroid responses to repeated ACTH administration of the 7 animals that participated in the experiment described by McCormley et al. 2018. LC-MS/MS sequencing yielded 137,926 MS/MS spectra, 15,387 peptide spectra matches (PSMs), and 8,793 proteins (with 1,260 protein groups) identified using the UniProt SwissProt database. We identified 564 proteins that had 2 or more unique peptides hits.

The collapsed protein isoform groups dataset containing 1,260 protein groups was used for subsequent functional annotation. Protein functional (KEGG) categories overrepresented in the elephant seal blubber proteome were identified using the DAVID functional annotation tool. Twenty-eight KEGG pathways were enriched ($p < 0.05$) in the proteome relative to the human genome background. The metabolic pathways category was the most significantly enriched and contained 48 elephant seal proteins. Other enriched pathways of interest included PI3K-Akt signaling (n=18 proteins), carbon metabolism (n=17), protein processing in E.R. (n=14), glycolysis/ gluconeogenesis (n=10), proteasome (n=10), biosynthesis of amino acids (n=9), RNA degradation (n=6), fatty acid metabolism (n=5), fatty acid degradation (n=5), and pyruvate metabolism (n=5), among others. These KEGG enrichment data were similar to those reported for elephant seal blubber transcriptomes [14, 28, 93].

Protein abundance was compared between sampling conditions using Proteome Discoverer 2.2. The numbers of differentially expressed proteins (DEPs) that were identified using the UniProt SwissProt reference database are shown in Table 3.1.

Table 3.1. Number of DEPs identified in each pairwise comparison

Comparison name	**Pairwise comparison**	**total DEPs***	**upreg. DEPs**	**downreg. DEPs**
First ACTH response	Day 1 ACTH response / Day 1 pre-ACTH	31	13	18
Fourth ACTH response	Day 4 ACTH response / Day 4 pre-ACTH	22	12	10
Overall ACTH response	Day 4 ACTH response / Day 1 pre-ACTH	27	9	18
Pre-ACTH comparison	Day 4 pre-ACTH / Day 1 pre-ACTH	11	5	6
ACTH response comparison	Day 4 ACTH response / Day 1 ACTH response	45	23	22

DEPs: differentially expressed proteins. DEPs*: Proteins identified with 2 or more unique peptides mapping back to identified protein in Uniprot Swissprot database and found in all sampling periods (pre-ACTH and post-ACTH administration on the first and fourth day.

The magnitude and significance of protein expression differences in each comparison are presented in Figures 2 and 3**.** We first examined changes in protein abundance over the course of the entire experiment (day 1 pre-ACTH vs. day 4 ACTH response; "overall ACTH response", in response to the first ACTH administration, fourth ACTH administration (Fig. 3.1). We then compared expression between day 1 and day 4 pre-ACTH conditions ("pre-ACTH comparison") and between day 1 and day 4 ACTH responses ("ACTH response comparison," (Fig. 3.2).

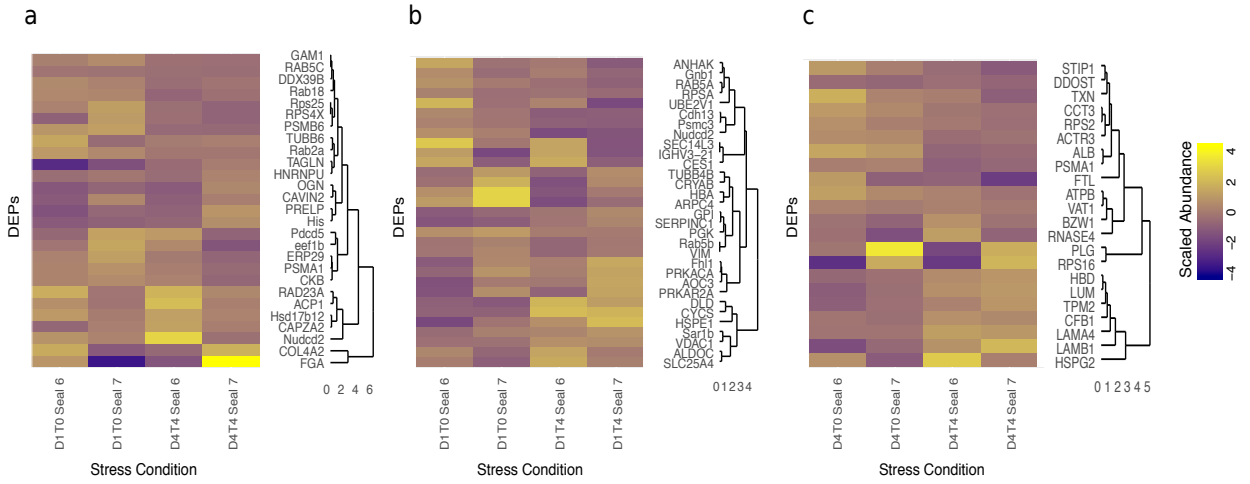

Figure 3.1. Heat map showing changes in scaled normalized protein abundance for differentially expressed proteins in the overall ACTH response (a), the first ACTH response (b), and the fourth ATCH response (c). DEPs are hierarchically clustered by expression levels. Upregulated and downregulated proteins that were significantly differentially expressed (p adj. <0.05) are shown in yellow and dark blue, respectively.

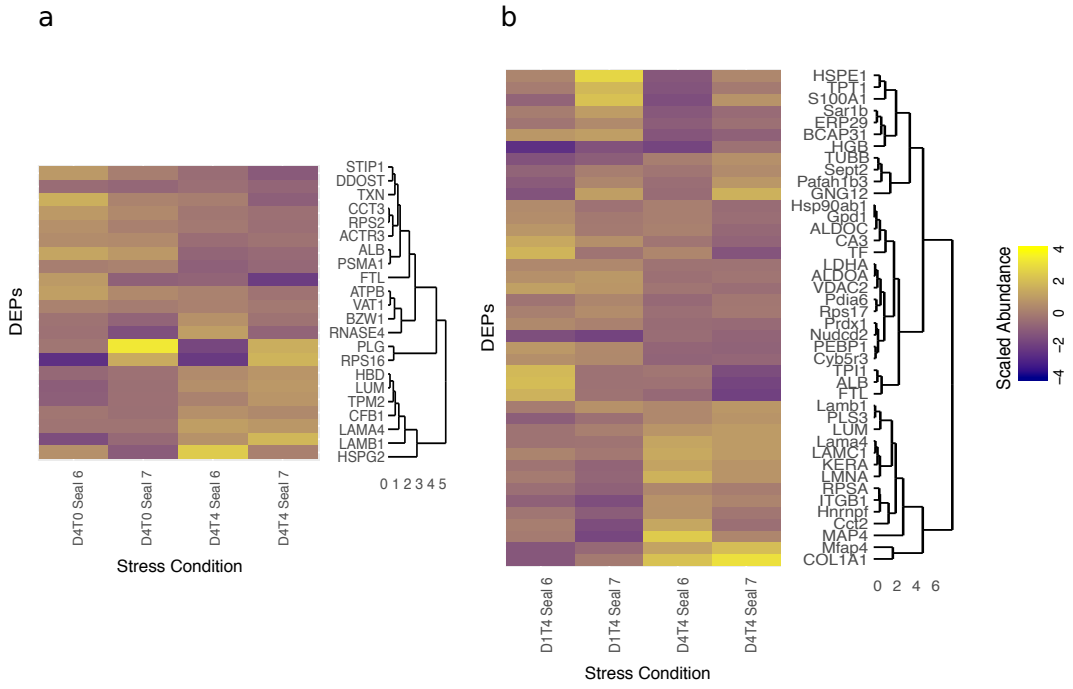

Figure 3.2. Heat map showing changes in scaled normalized protein abundance for differentially expressed proteins in the baseline comparison (a) and the ACTH response comparison (b). DEPs are hierarchically clustered by expression levels. Upregulated and downregulated proteins that were significantly differentially expressed (p adj. <0.05) are shown in yellow and dark blue, respectively.

Proteins were considered differentially expressed if their fold change between conditions was above 1.2 or below 0.8 (at adjusted $p < 0.05$). We identified 8 annotated, differentially expressed proteins (DEPs) covered by 2 or more unique peptides in response to the first ACTH administration, 7 DEPs in response to the fourth ACTH administration, 5 DEPs in the overall ACTH response, 1 DEP in the pre-ACTH comparison (Table 3.2), and 8 DEPs in the ACTH response comparison (Table 3.3).

Table 3.2. Proteins differentially expressed in the pre-ACTH comparison (between pre-ACTH samples from day 1 and pre-ACTH samples from day 4).

Protein ID	Uniprot Accession	Gene symbol	General function
Hypoxanthine-guanine phosphoribosyltransferase	P00493	HPRT1	purine nucleotide generation
Apolipoprotein A-I	P02648	APOA1	cholesterol transport
Annexin A6	P79134	ANXA6	calcium transport
Heat shock 70 kDa protein 1	Q7YQC6	HSPA1	protein chaperone
Proliferation-associated protein 2G4	Q9UQ80	PA2G4	growth regulation
Retinol binding protein 4	M5AXY1	RBP4	blood transport
78 kDa glucose-regulated protein	P11021	HSPA5	chaperone protein
60S ribosomal protein L3	P21531	RPL3	ribosomal protein
Receptor of activated protein C kinase 1	P68040	RACK1	signaling regulation
Hemoglobin subunit deltaH	Q45XI4	HGB	blood oxygen transport
Guanine nucleotide-binding protein G(s) subunit alpha isoforms XLas	Q63803	GNAS	guanine nucleotide binding

Table 3.3. Proteins differentially expressed in the ACTH response comparison (between ACTH response samples from day 1 and ACTH response samples from day 4).

Protein ID	Uniprot Accession	Gene symbol	General function
Integrin beta-1	A5Z1X6	ITGB1	cell adhesion
Plastin-3	A7E3Q8	PLS3	actin binding protein
40S ribosomal protein SA	B5FXT6	RPSA	ribosomal protein
Collagen alpha-1(I) chain	C0HJN3	COL1A1	extracellular matrix
Collagen alpha-1(I) chain	C0HJP7	COL1A1	extracellular matrix
Platelet-activating factor acetylhydrolase IB subunit gamma	O35263	Pafah1b3	brain development
Lumican	O46379	LUM	collagen binding

Keratocan	O62702	KERA	eye protein
Laminin subunit beta-1	P02469	Lamb1	extracellular matrix
Prelamin-A/C	P02545	LMNA	nuclear structure stability
Laminin subunit gamma-1	P11047	LAMC1	extracellular matrix
Hemoglobin subunit alpha-1/2	P20243	HBB	blood oxygen transport
Microtubule-associated protein 4	P27816	MAP4	microtubule assembly
Septin-2	P42208	Sept2	cytoskeletal GTPase
Lumican	P51884	LUM	collagen binding
T-complex protein 1 subunit beta	P80314	Cct2	ER stress
Laminin subunit alpha-4	P97927	Lama4	extracellular matrix
Prelamin-A/C	Q3ZD69	LMNA	nuclear structure stability
Tubulin beta chain	Q4P235	TUBB	microtubule protein
NudC domain-containing protein 2	Q5M823	Nudcd2	dynein pathway stablization
Heterogeneous nuclear ribonucleoprotein F	Q5RBQ0	GNG12	transmembrane signalling
Heterogeneous nuclear ribonucleoprotein F	Q794E4	Hnrnpf	RNA binding
Microfibril-associated glycoprotein 4	Q9D1H9	Mfap4	cell adhesion
Serum albumin	A2V9Z4	ALB	blood carrier protein
Translationally-controlled tumor protein	A5A6K2	TPT1	cell proliferation
Glycerol-3-phosphate dehydrogenase [NAD(+)], cytoplasmic	O35077	Gpd1	carbohydrate metabolism
Fructose-bisphosphate aldolase A	P00883	ALDOA	carbohydrate metabolism
Protein S100-A1	P02639	S100A1	cell cycle
40S ribosomal protein S17	P04644	Rps17	ribosomal protein
Carbonic anhydrase 3	P04644	CA3	catalysis of hydration on CO_2
Fructose-bisphosphate aldolase	P09972	ALDOC	carbohydrate metabolism
Heat shock protein HSP 90-beta	P11499	Hsp90ab1	heat shock chaperone protein
L-lactate dehydrogenase A chain	P19858	LDHA	anaerobic metabolism
NADH-cytochrome b5 reductase 3	P20070	Cyb5r3	electron transfer protein
Serotransferrin	P27425	TF	metal binding transport protein
Endoplasmic reticulum resident protein 29	P30040	ERP29	ER stress
Voltage-dependent anion-selective channel protein 2	P45880	VDAC2	mitochondrial membrane transport
Triosephosphate isomerase	P54714	TPI1	carbohydrate metabolism
10 kDa heat shock protein, mitochondrial	P61604	HSPE1	heat shock chaperone protein
Phosphatidylethanolamine-binding protein 1	Q3YIX4	PEBP1	serine protease inhibitor, ATP binding
Ferritin light chain	Q53VB8	FTL	iron storage protein
GTP-binding protein SAR1b	Q5HZY2	Sar1b	protein transport
B-cell receptor-associated protein 31	Q5R8H3	BCAP31	ER chaperone protein
Protein disulfide-isomerase A6	Q63081	Pdia6	ER stresss
Peroxiredoxin-1	Q63716	Prdx1	oxidatative stress

Manual UniProt database search was used to infer the functions of DEPs and predict their roles in blubber responses to single and repeated HPA axis activation. Proteins that were

upregulated (n=3) during the first ACTH response included cytochrome c (CYCS), a mitochondrial protein associated with the glycine cleavage system and alpha-ketoacid dehydrogenase complexes (DLD), and a mitochondrial protein chaperone (HSPE1). Cytochrome c was the most highly differentially expressed protein with an abundance ratio of 1.33. Proteins downregulated (n=5) during the first ACTH response had known functions in hydrophobic ligand binding and transport (SEC14L3), NF kappa B pathway activation (UBE2V1), and included an immunoglobin (IGHV3-21) and a HSP90 co-chaperone (NUDCD2). Proteins that were upregulated (n=7) in response to the fourth ACTH administration included extracellular matrix proteins (LUM, LAMB1, TPM2, LAMA4, HSPG2), one protein associated with RNA degradation (RNASE4), and a blood oxygen transport protein (HGB). Several proteins of interest that were downregulated in response to the fourth ACTH administration were identified as significantly different between conditions but were above the fold change threshold of 0.8. These included proteins with known roles in regulating interactions between HSP90 and other chaperones (STIP1), proteolytic degradation (PSMA1), protein folding (CCT), and cell redox homeostasis (TXN). In the overall ACTH response, upregulated proteins (n=5) were primarily associated with extracellular matrix (OGN, PRELP, TAGLN), wound healing (FGA), nucleic acid binding (HIS), and bone formation (OGN), while the only downregulated protein was translation elongation factor (EEF1B).

The only protein significantly upregulated in the pre-ACTH comparison was apolipoprotein APOA1, which is involved in cholesterol transport. Two proteins that were identified as significantly different between conditions (adj. $p < 0.05$), but had fold change values below and above the threshold, respectively – the purine salvage pathway enzyme HPRT1

(upregulated) and the adipokine RBP4 (downregulated) – have specific relevance to marine mammal physiology.

Proteins that were upregulated in the ACTH response comparison (n=7) were primarily associated with ECM and cell adhesion (e.g. COL1A1, ITGB1), nuclear structure stability (LMNA), and microtubule assembly and components (MAP4, TUBB). Proteins that were downregulated in the ACTH response comparison (n=3) were associated with protein folding (BCAP3) and iron homeostasis (FTL). Downregulated proteins of interest that were significantly different between conditions but had a fold change value above the threshold included carbonic anhydrase (CA3), NADH-cytochrome b5 reductase 3 (CYB5R3), a mitochondrial membrane channel protein (VDAC2), two glycolysis enzymes (TPI1, ALDOA), and an antioxidant protein (PRDX1).

Discussion

The overall goal of this study was to examine changes in global protein expression during blubber responses to single and repeated ACTH administration in a marine mammal. We previously showed that repeated ACTH administration (once daily for 4 days) induced significant elevation in corticosteroids (cortisol, aldosterone) and suppression of total triiodothyronine (T3) levels in juvenile elephant seals. However, the magnitude of the cortisol response did not vary between the first ("acute") and fourth ("repeated)" ACTH administration [1], highlighting the unreliability of using cortisol profiles alone for distinguishing stress states in wild animals. We therefore examined whether changes in expression of downstream targets of hormones – genes and proteins – differed between target tissue responses to single and repeated ACTH administration. We previously described the blubber transcriptome response to this experiment [93]. We found that genes associated with lipid droplet formation, lipolysis, and

fatty acid metabolism were upregulated in response to the fourth administration as compared to the first, while genes associated with adipogenesis, adipokine signaling, and fatty acid uptake were downregulated [93]. Other differentially expressed genes were associated with immune response, oxidative stress, glycolysis and carbohydrate metabolism, insulin resistance, and sensitivity to glucocorticoid hormones. In this study, we profiled changes in the blubber proteome as a complement to and a functional readout of endocrine and transcriptional responses to repeated ACTH administration.

Proteins that were upregulated in response to the first ACTH administration were cytochrome c (CYCS), dihydrolipoyl dehydrogenase, mitochondrial (DLD), and 10 kDa heat shock protein, mitochondrial (HSPE1). Cytochrome c, which has functions in the electron transport chain, apoptosis, and redox homeostasis, was the most highly upregulated protein in this comparison. Its upregulation is consistent with studies in other species that have shown increases in mitochondrial and metabolic activity and oxidative damage in response to stress [102, 103]. However, any potential oxidative damage may be countered by the innately high antioxidant capacity in these diving-adapted mammals [78], as well as by upregulation of antioxidant genes (e.g. GPX3) observed in response to ACTH administration in the same experiment [93]. DLD, which converts dihydrolipoic acid and NAD+ into lipoic acid and NADH [104], is associated with regulation of the tricarboxylic acid cycle and amino acid catabolism. In addition, DLD may function as an antioxidant due to its ability to scavenge nitric oxide and to reduce ubiquinone to ubiquinol [105]. Lastly, HSPE1 is a mitochondrial chaperone that is involved in mediating folding and assembly of mitochondrial protein complexes. Together, these upregulated proteins suggest that blubber responses to acute HPA axis activation include changes in mitochondrial function, with complex effects on energy metabolism and

redox homeostasis. Proteins that were downregulated in response to the first ACTH administration included those involved in hydrophobic ligand binding and transport (SEC14L3), protein ubiquitination (UBE2V1), protein folding (NUDCD2), and immune responses (IGHV3-21). UBE2V1 plays a role in NF-κB activation, SIRT1 inhibition [106], autophagy, cancer, and DNA repair [107]. Downregulation of UBE2V1 and IGHV3-21 is consistent with the anti-inflammatory effects of acute exposure to GCs and with the downregulation of pro-inflammatory genes observed in response to ACTH administration in elephant seals [14, 29, 93]. NUDCD2 is a co-chaperone of HSP90, which regulates glucocorticoid receptor function and translocation to the nucleus [108]. Its downregulation may potentially serve as a negative feedback mechanism to reduce HSP90 activity and decrease sensitivity to GCs during acute responses to HPA axis stimulation. This is consistent with upregulation of transcripts for NCOR1, a negative regulator of the GR gene, in response to ACTH administration in elephant seal blubber [93].

Proteins upregulated in response to the fourth ACTH administration were associated with RNA degradation (RNASE4), ECM function, a blood oxygen transport protein (HGB), and cell migration (LUM, LAMB1, LAMA4, HSPG2, TPM2). Basement membrane-specific heparan sulfate proteoglycan core protein (HSPG2), also known as perlecan, regulates adipose tissue metabolism [109] and interacts with low density lipoproteins [110]. Perlecan knockout mice have smaller adipose tissue mass, increased levels of fatty acid oxidation, and enhanced insulin sensitivity [109]. Upregulation of this protein in elephant seal blubber may limit beta-oxidation during responses to repeated HPA axis activation, potentially in order to conserve lipid stores, and may contribute to the insulin resistance observed in fasting-adapted marine mammals [31]. There were no proteins that were considered significantly downregulated (fold change < 0.8) in response to the fourth ACTH administration. However, some proteins with fold change values

between 0.8 and 0.99 were considered statistically significantly different (adj. $p < 0.05$) and were of interest to this study. These included another co-chaperone of HSP90 (STIP1) and an antioxidant (TXN). Therefore, the impacts of repeated HPA axis activation on GR activity and redox homeostasis in marine mammal tissues warrant further investigation.

Proteins upregulated in response to the entire experiment (day 4 ACTH response samples vs. day 1 pre-ACTH samples) were primarily associated with extracellular matrix function. One of the upregulated proteins, mimecan (OGN), is highly expressed in adipose in other mammals and has been shown to suppress food intake independently of leptin by inducing expression of interleukins (IL-1β and IL-6) in the hypothalamus [111, 112]. Mimecan is also upregulated in pituitary corticotroph cells of rats in response to GC treatment, suggesting that its expression may be mediated by GR [113, 114]. Interestingly, genes encoding other ECM proteins (e.g. collagen) were downregulated in blubber during fasting in elephant seals [61], despite modest elevation in cortisol levels [115]. Further investigation is needed to understand the role of OGN and other upregulated ECM proteins (prolargin, transgelin) in normal and stress-induced function in adipose tissue. However, it is also possible that upregulation of some proteins associated with wound healing (e.g. fibrinogen) may be an artefact of tissue responses to repeated biopsy sampling, rather than responses to ACTH. Only one protein was downregulated in the overall ACTH response, translation elongation factor 1 beta (EEF1B). EEF1B is upregulated by GCs in rat hepatocytes [116], but its expression in other cell types has not been examined. Its downregulation in seal blubber may serve to reduce energy expenditure associated with protein translation during repeated HPA axis activation.

We next compared protein expression between pre-ACTH samples collected on the fourth and first days. The only upregulated protein in this comparison was apolipoprotein A-I

(APOA1), which transports cholesterol from tissues to the liver for excretion. APOA1 is regulated by GCs [117] and has been shown to promote glucose uptake, adiponectin expression, and insulin sensitivity, and to decrease inflammation in adipocytes [118]. Apolipoprotein A-I has been shown to play a role in adipocyte metabolism by intracellular signaling activated by direct APOA1 surface receptor interactions. Interestingly, adiponectin transcripts were also upregulated in the pre-ACTH comparison [93], potentially as a consequence of upregulation of APOA1 protein. Therefore, APOA1 may mediate metabolic recovery from repeated ACTH administration via its effects on adipokine expression. There were no proteins that were downregulated (fold change < 0.8) in this comparison. Two proteins of interest to marine mammal physiology, hypoxanthine-guanine phosphoribosyl transferase (HGPRT, fold change: 1.053) and retinol binding protein 4 (RBP4, fold change: 0.94), did not meet the fold change cutoff but were considered significantly different between conditions (adj. $p<0.05$). HGPRT is involved in in purine recycling, which increases during apneas and prolonged fasting in elephant seals [119]. RBP4 is an adipokine that promotes insulin resistance [120] and has been associated with oxidative stress and inflammation [121]. RBP4 transcripts were upregulated in muscle tissue 24 hours after a single ACTH administration in juvenile northern elephant seals [29], suggesting a potential role in metabolic recovery from acute corticosteroid elevation. The role of these proteins in repeated HPA axis activation warrants further investigation.

Lastly, we assessed whether the blubber responses to single and repeated HPA axis activation were different by comparing protein expression between ACTH response samples collected on the fourth and first days. We identified 10 DEPs that met the fold change and significance cutoffs and 45 additional DEPs that met the statistical, but not the fold change cutoff. Seven proteins upregulated in day 4 ATCH response samples were associated with cell

adhesion, ECM function, and microtubule cytoskeleton dynamics. Increased ECM deposition and remodeling is associated with adipogenesis [94], which is stimulated by GCs. We found that some transcripts associated with adipogenesis were upregulated, while adipogenesis inhibitors were downregulated in elephant seal blubber in response to ACTH administration [14, 93]. Therefore, increased ECM synthesis may mirror an increase in adipogenesis during the response to repeated ACTH administration. Three proteins that were downregulated in day 4 ATCH response samples were serum albumin, ferritin light chain (FTL), and B-cell receptor-associated protein 31 (BCAP31). FTL has been associated with anti-inflammatory and antioxidant functions [122] and its expression is negatively correlated with adipogenesis and insulin resistance in human adipose tissue [123]. Therefore, downregulation of FTL is consistent with a potential increase in adipogenesis during blubber responses to repeated corticosteroid elevation. However, differential expression of FTL and albumin may be an artefact of biopsy sampling or variability in peripheral vasoconstriction in these diving-adapted mammals [124], and should be verified using a larger sample size. If FTL stimulates adipogenesis, this finding is consistent with transcriptome data, which showed that the adipogenesis inhibitor transforming growth factor beta-induced (TGFBI) was downregulated in the ACTH response comparison [93]. BCAP3 is an ER chaperone protein that is associated with protein secretion, Fas-activated apoptosis, and T cell proliferation and activation[125]; its downregulation is consistent with the immunosuppressive effect of chronic GC elevation. Several proteins that met the statistical, but not the fold change cutoff for downregulation (fold change between 0.8 and 0.9) were associated with glycolysis (ALDOA, TPI), cholesterol and fatty acid synthesis [126] (CYB5R3), and mitochondrial protein folding and membrane transport (HSPE1, VDAC2). VDAC2 has been associated with adipogenesis, steroidogenesis, and oxidative metabolism [127]. These data,

while tenuous, are consistent with concomitant downregulation of transcripts of genes associated with fatty acid uptake (THBS1) and oxidation (C1QTNF3) in the same cells [93].

In summary, these data suggest that repeated HPA axis activation in a marine mammal impacts the abundance of blubber tissue proteins that are associated with redox homeostasis, mitochondrial function, adipogenesis, lipid and carbohydrate metabolism, and inflammation. While we did not identify DEPs that matched differentially expressed transcripts (DEGs) in the same cells, the functions of DEPs overlapped with those of the DEGs identified in our recent transcriptome study [93]. These included the protein APOA1, which was upregulated in this study, and transcripts encoding genes involved in lipid metabolism and adipogenesis (e.g. adiponectin, leptin, ACSM1), which were upregulated in the transcriptome study [93]. However, both studies were limited by small sample size and short duration of experimental manipulation, producing fairly low numbers of significant DEGs and DEPs. Nevertheless, these data provide the first insights into functional consequences of repeated ("chronic") GC elevation in marine mammals and lay the foundation for future studies aimed at detecting stress states in these and potentially other animals. Due to the relative stability of proteins (compared to nucleic acids), and the ease of blubber sampling in some species (e.g. by remote dart biopsy), expression of proteins such as those identified in this study may help conservation biologists assess the impacts on chronic stress on threatened marine mammal populations. Lastly, these studies highlight the power of integrating endocrine, transcriptome, and proteome data for understanding the physiological impacts of repeated stress in animals.

Synthesis and Future Directions

The combination of transcriptomics and proteomics has provided a more comprehensive insight into acute and repeated stress responses in marine mammals than could be obtained by

each technique alone. Due to the inability of circulating cortisol levels to distinguish between acute and repeated stress states [1], I used the more sensitive approaches of transcriptome and proteome sequencing to capture changes in target gene and protein expression in blubber in response to single and repeated ACTH administration. Transcriptomics identified changes in expression of stress hormone target genes, while proteomics captured alterations in intracellular, secreted, and extracellular proteins in response to simulated physiological stress. Overall, both methods allowed for the identification of additional stress markers, as well as overlaps in function between differentially expressed transcripts and proteins.

I was able to detect similarities and differences in the transcriptome and proteome responses to single and multiple ACTH administrations (Fig. 3.3).

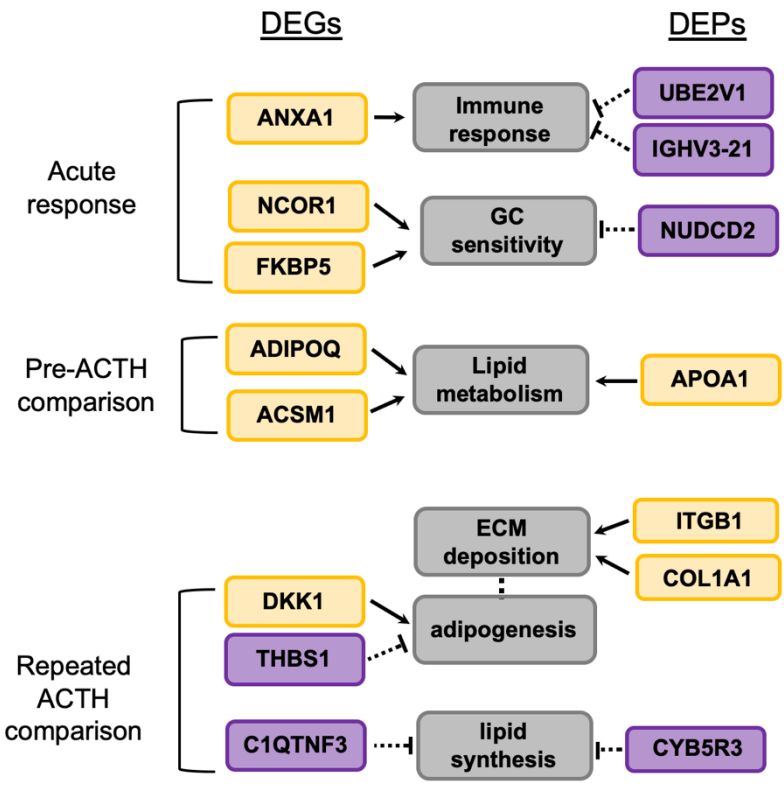

Figure 3.3. Significant differentially expressed genes and proteins with commonly shared functions in response to single and multiple ACTH administrations. DEGs are represented on the left side, shared functions in the middle, and DEPs on the right, respectively. Orange and purple depict upregulation or downregulation in expression, respectively. Upregulation of genes or proteins associated with a common function is shown by an arrow, whereas downregulation is shown to suppress the common function with a dotted line and a blunt ended arrow.

I found overlaps in known functions of DEGs and DEPs, many of which were associated with decreased immune signaling and negative feedback on the HPA axis in response to a single ACTH administration. Increases in expression of anti-inflammatory genes was correlated with decreases in expression of pro-inflammatory proteins, which is consistent with studies that have shown that stress causes a shift in energy allocation away from energetically demanding functions such as the immune response [128]. Upregulation of genes and proteins associated with negative regulation of glucocorticoid receptor signaling suggests that fasting-adapted marine mammals may be able to modify their sensitivity to lipolysis-promoting cortisol during acute

stress responses, potentially in order to conserve metabolic stores. Specifically, I saw an increase in expression of DEGs associated with negative regulation of the GR gene, while an HSP90 co-chaperone protein, which may cooperate with HSP90 to sequester GR in the cytosol and prevent its translocation to the nucleus, was downregulated [129]. In the pre-ACTH comparison, I detected changes in expression of genes and proteins associated with lipolysis, suggesting that repeated ACTH administration may cause alterations in adipose tissue metabolism that can be detected 24 hours after each injection, even after cortisol levels have returned to baseline levels [1]. This finding is consistent with the decline in circulating triacylglyceride levels observed in response to repeated ACTH administration in the same study animals [91], as well as the lipolytic effects of cortisol described in other species [10, 130]. In response to the fourth ACTH administration, genes and proteins associated with adipogenesis and ECM deposition were upregulated, while those associated with lipid synthesis were downregulated. This suggests that GC-induced adipogenesis may be accompanied by increased ECM remodeling, as has been shown in recent human and mouse studies [94, 131]. Decrease in expression of transcripts and proteins associated with lipid synthesis is consistent with the catabolic effects of cortisol. Overall, these findings suggest that repeated stress may alter lipid transport, storage, and metabolism, potentially altering energy homeostasis in marine mammals. In fasting-adapted species such as capital breeding marine mammals, this may lead to an overall decline in fitness as depletion of energy reserves will impact an animal's ability to sustain prolonged fasts associated with reproduction.

In summary, these two studies provided insights into the impacts of acute and repeated ACTH administration on gene and protein expression and potential metabolic pathways associated with DEGs and DEPs. Most importantly, I detected changes in blubber transcriptome

and proteome profiles to acute and repeated ACTH administration despite similarities in circulating hormone levels, highlighting the utility and sensitivity of omics approaches for detecting functional consequences of stress and identifying biomarkers that can be used to assess stress levels in vulnerable, endangered, or less accessible marine mammal populations.

Future studies could include validation of differentially expressed genes and proteins using targeted assays in a larger population of animals of unknown baseline stress states. The effects of single and repeated ACTH administration on gene and protein expression profiles in other glucocorticoid target tissues (e.g., muscle, an energy-utilizing tissue) should also be evaluated. Additionally, studying changes in stress markers identified in response to normal life history challenges is of future interest. These include evaluating changes in gene expression or protein abundance during fasting, reproduction, or molting to provide a baseline context against which to evaluate changes in response to unpredictable stress. Other future studies of interest could investigate if animals experiencing sustained stress can be identified based on variability in these molecular markers. Evaluating the effects of repeated HPA axis activation on oxidative stress load, global lipid and other metabolite profiles, and immune capacity using a variety of targeted and non-targeted assays (e.g. lipidomics and metabolomics) would also contribute towards a more comprehensive understanding of impacts of exposure to physiological stress on marine mammal physiology. Lastly, comparative studies using similar approaches to evaluate physiological impacts of stress in terrestrial mammals or other animals would provide a more comprehensive understanding of the unique physiological challenges and adaptations of marine mammals, and their ability to tolerate unpredictable global change.

References

1. McCormley, M.C., et al., *Repeated adrenocorticotropic hormone administration alters adrenal and thyroid hormones in free-ranging elephant seals.* Conserv Physiol, 2018. **6**(1): p. coy040.
2. Ceballos, G., et al., *Accelerated modern human-induced species losses: Entering the sixth mass extinction.* Sci Adv, 2015. **1**(5): p. e1400253.
3. Ripple, W.J., et al., *Status and ecological effects of the world's largest carnivores.* Science, 2014. **343**(6167): p. 1241484.
4. Springer, A.M., et al., *Sequential megafaunal collapse in the North Pacific Ocean: an ongoing legacy of industrial whaling?* Proc Natl Acad Sci U S A, 2003. **100**(21): p. 12223-8.
5. Maxwell, S.M., et al., *Cumulative human impacts on marine predators.* Nat Commun, 2013. **4**: p. 2688.
6. Davidson, A.D., et al., *Drivers and hotspots of extinction risk in marine mammals.* Proc Natl Acad Sci U S A, 2012. **109**(9): p. 3395-400.
7. Atkinson, S., D.P. Demaster, and D.G. Calkins, *Anthropogenic causes of the western steller sea lion eumetopias jubatus population decline and their threat to recovery.* Mammal Review, 2008. **38**: p. 1-18.
8. Kunc, H.P., K.E. McLaughlin, and R. Schmidt, *Aquatic noise pollution: implications for individuals, populations, and ecosystems.* Proc Biol Sci, 2016. **283**(1836).
9. Boonstra, R. and C. Fox, *Reality as the leading cause of stress: rethinking the impact of chronic stress in nature.* Functional Ecology, 2013. **27**(1): p. 11-23.
10. Sapolsky, R.M., L.M. Romero, and A.U. Munck, *How do glucocorticoids influence stress responses? Integrating permissive, suppressive, stimulatory, and preparative actions.* Endocr Rev, 2000. **21**(1): p. 55-89.
11. Champagne, C.D., et al., *Comprehensive endocrine response to acute stress in the bottlenose dolphin from serum, blubber, and feces.* Gen Comp Endocrinol, 2018.
12. Atkinson, S., et al., *Stress physiology in marine mammals: how well do they fit the terrestrial model?* J Comp Physiol B, 2015. **185**(5): p. 463-86.
13. Kadmiel, M. and J.A. Cidlowski, *Glucocorticoid receptor signaling in health and disease.* Trends Pharmacol Sci, 2013. **34**(9): p. 518-30.
14. Khudyakov, J.I., et al., *Blubber transcriptome response to acute stress axis activation involves transient changes in adipogenesis and lipolysis in a fasting-adapted marine mammal.* Sci Rep, 2017. **7**: p. 42110.
15. Breuner, C.W., S.H. Patterson, and T.P. Hahn, *In search of relationships between the acute adrenocortical response and fitness.* Gen Comp Endocrinol, 2008. **157**(3): p. 288-95.
16. Christiansen, J.J., et al., *Effects of cortisol on carbohydrate, lipid, and protein metabolism: studies of acute cortisol withdrawal in adrenocortical failure.* J Clin Endocrinol Metab, 2007. **92**(9): p. 3553-9.
17. Fujiwara, M. and H. Caswell, *Demography of the endangered North Atlantic right whale.* Nature, 2001. **414**(6863): p. 537-41.
18. Pirotta, E., et al., *Understanding the population consequences of disturbance.* Ecology and Evolution, 2018.

19. Breuner, C.W., B. Delehanty, and R. Boonstra, *Evaluating stress in natural populations of vertebrates: total CORT is not good enough.* Functional Ecology, 2013. **27**(1): p. 24-36.
20. Champagne, C., et al., *Fasting Physiology of the Pinnipeds: The Challenges of Fasting While Maintaining High Energy Expediture and Nutrient Delivery for Lactation* Comparative Physiology of Fasting, Starvation, and Food Limitation. 2012, Springer: Springer, Berlin, Heidelberg.
21. Boyd, I.L., *State-dependent fertility in pinnipeds: contrasting capital and income breeders.* Functional Ecology, 2000. **14**(5): p. 623-630.
22. Braithwaite, J.E., J.J. Meeuwig, and M.R. Hipsey, *Optimal migration energetics of humpback whales and the implications of disturbance.* Conserv Physiol, 2015. **3**(1): p. cov001.
23. Strandberg, U., et al., *Stratification, composition, and function of marine mammal blubber: the ecology of fatty acids in marine mammals.* Physiol Biochem Zool, 2008. **81**(4): p. 473-85.
24. Lee, M.J., et al., *Deconstructing the roles of glucocorticoids in adipose tissue biology and the development of central obesity.* Biochim Biophys Acta, 2014. **1842**(3): p. 473-81.
25. Champagne, C., et al., *Adrenal sensitivity to stress is maintained despite variation in baseline glucocorticoids in moulting seals.* Conserv Physiol, 2015. **3**(1): p. cov004.
26. Le Boeuf, B.J., J. Burney, and R. Laws, *Elephant Seals: Population Ecology, Behavior, and Physiology*. 1994: Univeristy of California Press.
27. Jelincic, J.A., et al., *Variation in adrenal and thyroid hormones with life-history stage in juvenile northern elephant seals (Mirounga angustirostris).* Gen Comp Endocrinol, 2017. **252**: p. 111-118.
28. Khudyakov, J.I., et al., *Transcriptome analysis of northern elephant seal (Mirounga angustirostris) muscle tissue provides a novel molecular resource and physiological insights.* BMC Genomics, 2015. **16**: p. 64.
29. Khudyakov, J.I., et al., *Muscle transcriptome response to ACTH administration in a free-ranging marine mammal.* Physiol Genomics, 2015. **47**(8): p. 318-30.
30. Crocker, D.E., et al., *Adiposity and fat metabolism in lactating and fasting northern elephant seals.* Adv Nutr, 2014. **5**(1): p. 57-64.
31. Houser, D.S., C.D. Champagne, and D.E. Crocker, *A non-traditional model of the metabolic syndrome: the adaptive significance of insulin resistance in fasting-adapted seals.* Front Endocrinol (Lausanne), 2013. **4**: p. 164.
32. Champagne, C.D., et al., *The effects of handling and anesthetic agents on the stress response and carbohydrate metabolism in northern elephant seals.* PLoS One, 2012. **7**(5): p. e38442.
33. Oliver, S.G., et al., *Model organism databases: essential resources that need the support of both funders and users.* BMC Biol, 2016. **14**: p. 49.
34. Gladfelter, A.S., *How nontraditional model systems can save us.* Mol Biol Cell, 2015. **26**(21): p. 3687-9.
35. Russell, J.J., et al., *Non-model model organisms.* BMC Biol, 2017. **15**(1): p. 55.
36. Lindstedt, S., *Krogh 1929 or 'the Krogh principle'.* J Exp Biol, 2014. **217**(Pt 10): p. 1640-1.
37. Collins, L.J., et al., *An approach to transcriptome analysis of non-model organisms using short-read sequences.* Genome Inform, 2008. **21**: p. 3-14.

38. Costa-Silva, J., D. Domingues, and F.M. Lopes, *RNA-Seq differential expression analysis: An extended review and a software tool.* PLoS One, 2017. **12**(12): p. e0190152.
39. Manzoni, C., et al., *Genome, transcriptome and proteome: the rise of omics data and their integration in biomedical sciences.* Brief Bioinform, 2018. **19**(2): p. 286-302.
40. Steinberg, J., et al., *Integrative epigenomics, transcriptomics and proteomics of patient chondrocytes reveal genes and pathways involved in osteoarthritis.* Sci Rep, 2017. **7**(1): p. 8935.
41. Haider, S. and R. Pal, *Integrated analysis of transcriptomic and proteomic data.* Curr Genomics, 2013. **14**(2): p. 91-110.
42. Maier, T., M. Guell, and L. Serrano, *Correlation of mRNA and protein in complex biological samples.* FEBS Lett, 2009. **583**(24): p. 3966-73.
43. Kelso, E.J., et al., *Sex differences in fuel use and metabolism during development in fasting juvenile northern elephant seals.* J Exp Biol, 2012. **215**(Pt 15): p. 2637-45.
44. Chen, E.A., et al., *Effect of RNA integrity on uniquely mapped reads in RNA-Seq.* BMC Res Notes, 2014. **7**: p. 753.
45. Towns, J., et al., *XSEDE: Accelerating Scientific Discovery.* Computing in Science & Engineering, 2014. **16**(5): p. 62-74.
46. Haas, B.J., et al., *De novo transcript sequence reconstruction from RNA-seq using the Trinity platform for reference generation and analysis.* Nat Protoc, 2013. **8**(8): p. 1494-512.
47. Leggett, R.M., et al., *Sequencing quality assessment tools to enable data-driven informatics for high throughput genomics.* Front Genet, 2013. **4**: p. 288.
48. Langmead, B. and S.L. Salzberg, *Fast gapped-read alignment with Bowtie 2.* Nat Methods, 2012. **9**(4): p. 357-9.
49. Simao, F.A., et al., *BUSCO: assessing genome assembly and annotation completeness with single-copy orthologs.* Bioinformatics, 2015. **31**(19): p. 3210-2.
50. Buchfink, B., C. Xie, and D.H. Huson, *Fast and sensitive protein alignment using DIAMOND.* Nat Methods, 2015. **12**(1): p. 59-60.
51. Grabherr, M.G., et al., *Full-length transcriptome assembly from RNA-Seq data without a reference genome.* Nat Biotechnol, 2011. **29**(7): p. 644-52.
52. Wang, S.S., et al., *Gdf6 induces commitment of pluripotent mesenchymal C3H10T1/2 cells to the adipocyte lineage.* FEBS J, 2013. **280**(11): p. 2644-51.
53. Benjamini, Y. and Y. Hochberg, *Controlling The False Discovery Rate - A Practical And Powerful Approach To Multiple Testing.* J. Royal Statist. Soc., Series B, 1995. **57**.
54. Bray, N.L., et al., *Near-optimal probabilistic RNA-seq quantification.* Nat Biotechnol, 2016. **34**(5): p. 525-7.
55. Anders, S. and W. Huber, *Differential expression analysis for sequence count data.* Genome Biol, 2010. **11**(10): p. R106.
56. Szklarczyk, D., et al., *The STRING database in 2017: quality-controlled protein-protein association networks, made broadly accessible.* Nucleic Acids Res, 2017. **45**(D1): p. D362-D368.
57. Shannon, P., et al., *Cytoscape: a software environment for integrated models of biomolecular interaction networks.* Genome Res, 2003. **13**(11): p. 2498-504.
58. Conesa, A., et al., *A survey of best practices for RNA-seq data analysis.* Genome Biol, 2016. **17**: p. 13.

59. Honaas, L.A., et al., *Selecting Superior De Novo Transcriptome Assemblies: Lessons Learned by Leveraging the Best Plant Genome.* PLoS One, 2016. **11**(1): p. e0146062.
60. Oshlack, A. and M.J. Wakefield, *Transcript length bias in RNA-seq data confounds systems biology.* Biol Direct, 2009. **4**: p. 14.
61. Martinez, B., et al., *Adipose Transcriptome Analysis Provides Novel Insights into Molecular Regulation of Prolonged Fasting in Northern Elephant Seal Pups.* Physiol Genomics, 2018.
62. Oakley, R.H. and J.A. Cidlowski, *The biology of the glucocorticoid receptor: new signaling mechanisms in health and disease.* J Allergy Clin Immunol, 2013. **132**(5): p. 1033-44.
63. Gomez-Sanchez, E. and C.E. Gomez-Sanchez, *The Multifaceted Mineralocorticoid Receptor.* Comprehensive Physiology, 2014. **4**(3): p. 965-994.
64. Iwen, K.A.H., et al., *Melanocortin crosstalk with adipose functions: ACTH directly induces insulin resistance, promotes a pro-inflammatory adipokine profile and stimulates UCP-1 in adipocytes.* Journal of Endocrinology, 2008. **196**(3): p. 465-472.
65. Zamani, N. and C.W. Brown, *Emerging roles for the transforming growth factor-{beta} superfamily in regulating adiposity and energy expenditure.* Endocr Rev, 2011. **32**(3): p. 387-403.
66. Christodoulides, C., et al., *Adipogenesis and WNT signalling.* Trends Endocrinol Metab, 2009. **20**(1): p. 16-24.
67. Plaisier, C.L., et al., *Zbtb16 has a role in brown adipocyte bioenergetics.* Nutr Diabetes, 2012. **2**: p. e46.
68. Morey, J.N., et al., *Current Directions in Stress and Human Immune Function.* Curr Opin Psychol, 2015. **5**: p. 13-17.
69. Ensminger, D.C., et al., *Metabolic responses to adrenocorticotropic hormone (ACTH) vary with life-history stage in adult male northern elephant seals.* Gen Comp Endocrinol, 2014. **204**: p. 150-7.
70. Bali, U., et al., *FKBP5 mRNA Expression Is a Biomarker for GR Antagonism.* Journal of Clinical Endocrinology & Metabolism, 2016. **101**(11): p. 4305-4312.
71. Guo, X., et al., *DYRK1A and DYRK3 promote cell survival through phosphorylation and activation of SIRT1.* J Biol Chem, 2010. **285**(17): p. 13223-32.
72. Ramamoorthy, S. and J.A. Cidlowski, *Ligand-induced repression of the glucocorticoid receptor gene is mediated by an NCoR1 repression complex formed by long-range chromatin interactions with intragenic glucocorticoid response elements.* Mol Cell Biol, 2013. **33**(9): p. 1711-22.
73. Francisco, V., et al., *Obesity, Fat Mass and Immune System: Role for Leptin.* Front Physiol, 2018. **9**: p. 640.
74. Crocker, D.E., et al., *Hormone and metabolite changes associated with extended breeding fasts in male northern elephant seals (Mirounga angustirostris).* Comp Biochem Physiol A Mol Integr Physiol, 2012. **161**(4): p. 388-94.
75. Macfarlane, D.P., S. Forbes, and B.R. Walker, *Glucocorticoids and fatty acid metabolism in humans: fuelling fat redistribution in the metabolic syndrome.* J Endocrinol, 2008. **197**(2): p. 189-204.
76. John, K., et al., *The glucocorticoid receptor: cause of or cure for obesity?* Am J Physiol Endocrinol Metab, 2016. **310**(4): p. E249-57.

77. Spiers, J.G., et al., *Activation of the hypothalamic-pituitary-adrenal stress axis induces cellular oxidative stress.* Front Neurosci, 2014. **8**: p. 456.
78. Crocker, D.E., J.I. Khudyakov, and C.D. Champagne, *Oxidative stress in northern elephant seals: Integration of omics approaches with ecological and experimental studies.* Comp Biochem Physiol A Mol Integr Physiol, 2016. **200**: p. 94-103.
79. Konige, M., H. Wang, and C. Sztalryd, *Role of adipose specific lipid droplet proteins in maintaining whole body energy homeostasis.* Biochim Biophys Acta, 2014. **1842**(3): p. 393-401.
80. Hochberg, I., et al., *Gene expression changes in subcutaneous adipose tissue due to Cushing's disease.* Journal of Molecular Endocrinology, 2015. **55**(2): p. 81-94.
81. Barclay, J.L., et al., *Effects of glucocorticoids on human brown adipocytes.* Journal of Endocrinology, 2015. **224**(2): p. 139-147.
82. Brasaemle, D.L. and N.E. Wolins, *Packaging of fat: an evolving model of lipid droplet assembly and expansion.* J Biol Chem, 2012. **287**(4): p. 2273-9.
83. Lopez, Y.R., et al., *Effect of Glycine on Adipocyte Hypertrophy in a Metabolic Syndrome Rat Model.* Current Drug Delivery, 2016. **13**(1): p. 158-169.
84. Gopalakrishnan, K., et al., *Targeted disruption of Adamts16 gene in a rat genetic model of hypertension.* Proceedings of the National Academy of Sciences of the United States of America, 2012. **109**(50): p. 20555-20559.
85. Sun, L., et al., *Protein inhibitor of activated STAT 4 (PIAS4) regulates pro-inflammatory transcription in hepatocytes by repressing SIRT1.* Oncotarget, 2016. **7**(28): p. 42892-42903.
86. Yan, Y., et al., *SUMOylation of AMPKalpha1 by PIAS4 specifically regulates mTORC1 signalling.* Nat Commun, 2015. **6**: p. 8979.
87. Tews, D., et al., *Comparative gene array analysis of progenitor cells from human paired deep neck and subcutaneous adipose tissue.* Mol Cell Endocrinol, 2014. **395**(1-2): p. 41-50.
88. Kong, P., et al., *Thrombospondin-1 regulates adiposity and metabolic dysfunction in diet-induced obesity enhancing adipose inflammation and stimulating adipocyte proliferation.* Am J Physiol Endocrinol Metab, 2013. **305**(3): p. E439-50.
89. Li, Y., G.L. Wright, and J.M. Peterson, *C1q/TNF-Related Protein 3 (CTRP3) Function and Regulation.* Compr Physiol, 2017. **7**(3): p. 863-878.
90. Ehrlund, A., et al., *Transcriptional Dynamics During Human Adipogenesis and Its Link to Adipose Morphology and Distribution.* Diabetes, 2017. **66**(1): p. 218-230.
91. Champagne, C., et al. *Metabolic Response to Acute and Repeated Stress in Northern Elephant Seals*. in *Society for Marine Mammalogy* 2017.
92. Crocker, D.E., et al., *Maternal traits and reproductive effort in northern elephant seals.* Ecology, 2001. **82**(12): p. 3541-3555.
93. Deyarmin, J.S., et al., *Blubber transcriptome responses to repeated ACTH administration in a marine mammal.* Sci Rep, 2019. **9**(1): p. 2718.
94. Mariman, E.C. and P. Wang, *Adipocyte extracellular matrix composition, dynamics and role in obesity.* Cell Mol Life Sci, 2010. **67**(8): p. 1277-92.
95. Khudyakov, J.I., et al., *A sample preparation workflow for adipose tissue shotgun proteomics and proteogenomics.* Biol Open, 2018. **7**(11).
96. Huang da, W., B.T. Sherman, and R.A. Lempicki, *Systematic and integrative analysis of large gene lists using DAVID bioinformatics resources.* Nat Protoc, 2009. **4**(1): p. 44-57.

97. Zhu, M., et al., *Functional differentiation of Brassica napus guard cells and mesophyll cells revealed by comparative proteomics.* Mol Cell Proteomics, 2009. **8**(4): p. 752-66.
98. Chu, P., et al., *Data for iTRAQ-based quantitative proteomics analysis of Brassica napus leaves in response to chlorophyll deficiency.* Data Brief, 2015. **2**: p. 6-11.
99. Chen, T., et al., *iTRAQ-Based Quantitative Proteomic Analysis of Cotton Roots and Leaves Reveals Pathways Associated with Salt Stress.* PLoS One, 2016. **11**(2): p. e0148487.
100. Moulder, R., et al., *Quantitative proteomics analysis of the nuclear fraction of human CD4+ cells in the early phases of IL-4-induced Th2 differentiation.* Mol Cell Proteomics, 2010. **9**(9): p. 1937-53.
101. Cui, K., et al., *iTRAQ-based quantitative proteomic analysis of alterations in the intestine of Hu sheep under weaning stress.* PLoS One, 2018. **13**(7): p. e0200680.
102. Du, J., et al., *Dynamic regulation of mitochondrial function by glucocorticoids.* Proc Natl Acad Sci U S A, 2009. **106**(9): p. 3543-8.
103. Picard, M., et al., *An energetic view of stress: Focus on mitochondria.* Front Neuroendocrinol, 2018. **49**: p. 72-85.
104. Carothers, D.J., G. Pons, and M.S. Patel, *Dihydrolipoamide dehydrogenase: functional similarities and divergent evolution of the pyridine nucleotide-disulfide oxidoreductases.* Arch Biochem Biophys, 1989. **268**(2): p. 409-25.
105. Xia, L., et al., *Reduction of ubiquinone by lipoamide dehydrogenase. An antioxidant regenerating pathway.* Eur J Biochem, 2001. **268**(5): p. 1486-90.
106. Shen, T., et al., *Ube2v1-mediated ubiquitination and degradation of Sirt1 promotes metastasis of colorectal cancer by epigenetically suppressing autophagy.* J Hematol Oncol, 2018. **11**(1): p. 95.
107. Thomson, T.M., et al., *Role of UEV-1A, a homologue of the tumor suppressor protein TSG101, in protection from DNA damage.* FEBS Lett, 1998. **423**(1): p. 49-52.
108. Kirschke, E., et al., *Glucocorticoid receptor function regulated by coordinated action of the Hsp90 and Hsp70 chaperone cycles.* Cell, 2014. **157**(7): p. 1685-97.
109. Yamashita, Y., et al., *Perlecan, a heparan sulfate proteoglycan, regulates systemic metabolism with dynamic changes in adipose tissue and skeletal muscle.* Sci Rep, 2018. **8**(1): p. 7766.
110. Xu, Y.X., et al., *The glycosylation-dependent interaction of perlecan core protein with LDL: implications for atherosclerosis.* J Lipid Res, 2015. **56**(2): p. 266-76.
111. Cao, H.M., et al., *Mimecan, a Hormone Abundantly Expressed in Adipose Tissue, Reduced Food Intake Independently of Leptin Signaling.* EBioMedicine, 2015. **2**(11): p. 1718-24.
112. Harris, R.B., *Direct and indirect effects of leptin on adipocyte metabolism.* Biochim Biophys Acta, 2014. **1842**(3): p. 414-23.
113. Ma, Q.Y., et al., *Glucocorticoid up-regulates mimecan expression in corticotroph cells.* Mol Cell Endocrinol, 2010. **321**(2): p. 239-44.
114. Zhang, X.N., et al., *The mechanism of mimecan transcription induced by glucocorticoid in pituitary corticotroph cells.* Mol Cell Biochem, 2012. **360**(1-2): p. 321-8.
115. Ortiz, R.M., C.E. Wade, and C.L. Ortiz, *Effects of prolonged fasting on plasma cortisol and TH in postweaned northern elephant seal pups.* Am J Physiol Regul Integr Comp Physiol, 2001. **280**(3): p. R790-5.

116. Ayyar, V.S., et al., *Functional proteomic analysis of corticosteroid pharmacodynamics in rat liver: Relationship to hepatic stress, signaling, energy regulation, and drug metabolism.* J Proteomics, 2017. **160**: p. 84-105.
117. Mooradian, A.D., M.J. Haas, and N.C. Wong, *Transcriptional control of apolipoprotein A-I gene expression in diabetes.* Diabetes, 2004. **53**(3): p. 513-20.
118. Wang, S., D.Q. Peng, and Y. Yi, *The unsolved mystery of apoA-I recycling in adipocyte.* Lipids Health Dis, 2016. **15**: p. 35.
119. Sonanez-Organis, J.G., et al., *Prolonged fasting increases purine recycling in post-weaned northern elephant seals.* J Exp Biol, 2012. **215**(Pt 9): p. 1448-55.
120. Yang, Q., et al., *Serum retinol binding protein 4 contributes to insulin resistance in obesity and type 2 diabetes.* Nature, 2005. **436**(7049): p. 356-62.
121. Liu, Y., et al., *Associations of retinol-binding protein 4 with oxidative stress, inflammatory markers, and metabolic syndrome in a middle-aged and elderly Chinese population.* Diabetol Metab Syndr, 2014. **6**(1): p. 25.
122. Fan, Y., et al., *The effect of anti-inflammatory properties of ferritin light chain on lipopolysaccharide-induced inflammatory response in murine macrophages.* Biochim Biophys Acta, 2014. **1843**(11): p. 2775-83.
123. Moreno-Navarrete, J.M., et al., *Insulin resistance modulates iron-related proteins in adipose tissue.* Diabetes Care, 2014. **37**(4): p. 1092-100.
124. Blix, S.B. and B. Folkow, *Cardiovascular Adjustments to Diving in Mammals and Birds.* Compr Physiol, 2011. **Supplement 8**(Handbook of Physiology, The Cardiovascular System, Peripheral Circulation and Organ Blood Flow): p. 917-945.
125. Niu, K.W., et al., *BAP31 is involved in T cell activation through TCR signal pathways.* Scientific Reports, 2017. **7**.
126. Martin-Montalvo, A., et al., *Cytochrome b5 reductase and the control of lipid metabolism and healthspan.* NPJ Aging Mech Dis, 2016. **2**: p. 16006.
127. Naghdi, S. and G. Hajnoczky, *VDAC2-specific cellular functions and the underlying structure.* Biochim Biophys Acta, 2016. **1863**(10): p. 2503-14.
128. Coutinho, A.E. and K.E. Chapman, *The anti-inflammatory and immunosuppressive effects of glucocorticoids, recent developments and mechanistic insights.* Mol Cell Endocrinol, 2011. **335**(1): p. 2-13.
129. Echeverria, P.C., et al., *Nuclear import of the glucocorticoid receptor-hsp90 complex through the nuclear pore complex is mediated by its interaction with Nup62 and importin beta.* Mol Cell Biol, 2009. **29**(17): p. 4788-97.
130. Wang, J.C., et al., *Regulation of triglyceride metabolism by glucocorticoid receptor.* Cell Biosci, 2012. **2**(1): p. 19.
131. Mori, S., et al., *Characteristic expression of extracellular matrix in subcutaneous adipose tissue development and adipogenesis; comparison with visceral adipose tissue.* Int J Biol Sci, 2014. **10**(8): p. 825-33.